University (2006362). Every effort was made to optimize the comfort and to minimize the use of animals. According to our previous report [31], the cultured primary cortical neurons were prepared. Briefly, the cerebral cortex was dissected and cut into small pieces in Hanks' balanced salt solution (HBSS: Ca^{2+} and Mg^{2+} free) (Invitrogen, Carlsbad, CA, USA). The tissue was then dispersed with 0.025% trypsin-EDTA solutions (Invitrogen, Carlsbad, CA USA). The cell suspension was centrifuged at 800 × *g* for 5 min. The cells were suspended in Neurobasal Medium (Invitrogen, Carlsbad, CA, USA) supplemented with 2% of B27 containing antioxidants (Invitrogen, Carlsbad, CA, USA), L-glutamine (final concentration 0.5 mM) and antibiotic–antimycotic solution (final concentration 1%) (Nacalai tesque, Kyoto, Japan). The cell suspension was centrifuged at 800 × *g* for 5 min. Live cells were counted using a hemocytometer, and the cell suspension was then diluted with Neurobasal Medium at 2×10^6 cells/ml. Cells were seeded onto poly-D-lysine-coated 6-well plates (BD Bioscience, Discovery Labware, Bedford, MA, USA) in 2×10^6 cells/ml well. All cultures were maintained in Neurobasal Medium at 37 °C in 95% humidified air and 5% CO_2. At the 3rd day of culture, cytosine β-D-arabino-furanoside hydrochloride (final concentration 10 μM) (Sigma, St. Louis, MO, USA), a selective inhibitor of DNA synthesis, was added for 72 h in culture to prevent further proliferation of non-neuronal cells.

Orexin-A, orexin-B and MCH (0.01, 0.1 and 1 μM) were applied to cultured wells on the 6th day of culture, and the cultured cells were incubated for 6 days. Cultured medium which contained neuropeptides was changed every 3 days. On the 12th day of culture, the total cellular RNA was extracted from two cultured wells as one RNA sample using an RNeasy Mini Kit (Quiagen Sciences, MA, USA). The samples were stored at −20 °C until assay. All experiments consisted of three to six repetitive runs. For each experiment, two to six mRNA were obtained. Orexin-A, orexin-B and MCH were purchased from Peptide Institute Inc. (Osaka, Japan). Neuronal degeneration was assessed every 3 days after neuropeptide application using the efflux of lactate dehydrogenase by CytoTox 96® Non-Radioactive Cytotoxicity Assay (Promega Co., Madison, WI, USA) [31].

Quantitative real-time RT-PCR was conducted according to our previous report [31]. Quantitative real-time RT-PCR was performed with the ABI PRISM 7500 instrument (Applied Biosystems, Foster City, CA, USA) using SYBR green dye. Quantitative PCR was conducted in duplicate with 50 μl of reaction mixture in MicroAmp optical 96-well reaction plates. Each reaction well contained 12.5 μl of RNA sample, 25 μl of SYBR Green PCR Master Mix, 0.5 μl of RT Mix (Quiagen Sciences, MA, USA), 7 μl RNAase free water, and 25 pmol each of forward and reverse primers. Primers for glyceraldehyde-3-phosphate dehydrogenase (GAPDH) were as follows: [sense 5′-TGCACCACCAACTGCTTAGC-3′, antisense 5′-GGATGCAGGGATGATGTTCTG-3′], for OX1R, [sense 5′-GCATATCCACCTGGCCTGAA-3′, antisense 5′-CCACCATGCCAACGAGATCC-3′] [28], for OX2R, [sense 5′-CTACGCTCTTCTGCTATTGA-3′, antisense 5′-ACTGGCATGCTGATACATAC-3′] [28], for MCHR1, [sense 5′-TCA GCT TGG GCT ATG CTA ACA G-3′, antisense 5′-CAA CAC CAA GCG TTT TCG AA-3′ [8], for BDNF, [sense 5′-GGTCACAGTCCTGGAGAAAG-3′, antisense 5′-GCTTATCCTTATGAACCGCC-3] [30], and for NT-3, [sense 5′-TGCAGAGCATAAGAGTCACC-3′, antisense 5′-AAGTCAGTGCTCGGACGTAG-3′] [30]. All gene-specific mRNA expression values were normalized against the internal housekeeping gene GAPDH.

The results are presented as the mean ± S.E.M. of 8–31 RNA samples per group. Statistical analysis of the data was carried out by analysis of variance (ANOVA) followed by Dunnett's multiple range test. Statistical significance was defined as $p < 0.05$.

Quantitative RT-PCR analysis showed the presence of mRNAs of orexin receptors (OXR1, OXR2) and MCH receptor (MCHR1) in rat primary cortical neuron cultures used in this study (Fig. 1). Moreover, the basal expressions of NT-3 and BDNF mRNAs were also detected in the cultured cortical neurons (Fig. 2).

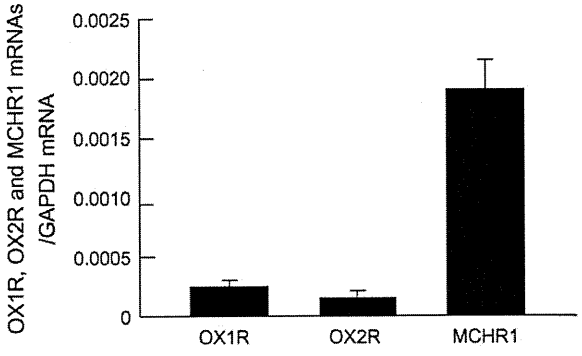

Fig. 1. mRNA expressions of orexin receptors (OX1R, OX2R) and MCHR1 in rat cultured cortical neurons. The values are mean ± S.E.M. from 9 to 10 RNA samples.

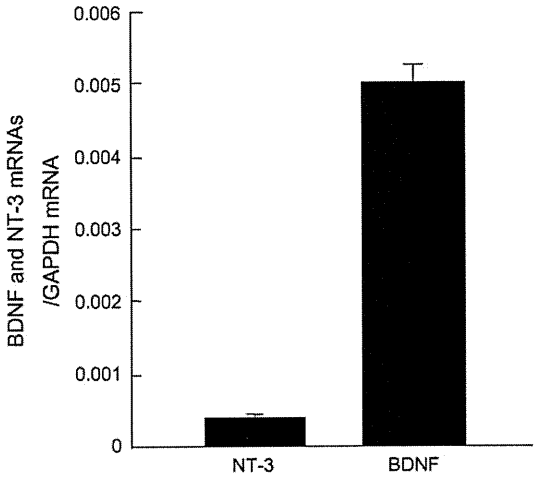

Fig. 2. mRNA expressions of BDNF and NT-3 in rat cultured cortical neurons. The values are mean ± S.E.M. from 8 to 31 RNA samples.

The mRNA expression of NT-3 following 6-day exposure to orexin-A at 0.01, 0.1 and 1 μM markedly increased to 1.57, 1.84 and 2.31 of control levels, respectively (Fig. 3). In a similar manner, orexin-B at 0.01, 0.1 and 1 μM also led to significant increases to 1.55, 1.63 and 2.49-fold of the control levels, respectively (Fig. 3).

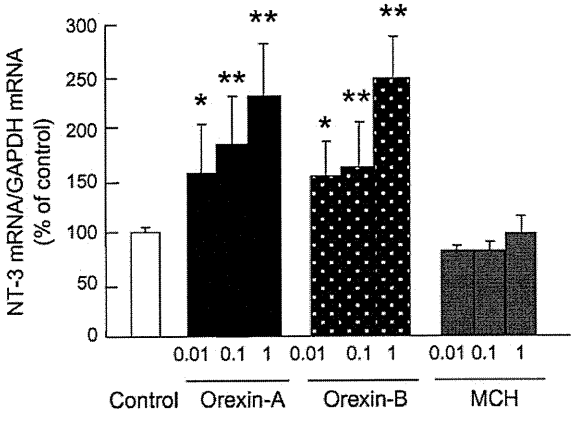

Fig. 3. Changes of mRNA expression of NT-3 induced by incubation for 6 days with orexin-A, orexin-B and MCH (0.01, 0.1, and 1 μM). Data are presented as a percentage of the control. The values are mean ± S.E.M. from 11 RNA samples. *$p < 0.05$, **$p < 0.01$ vs. control group.

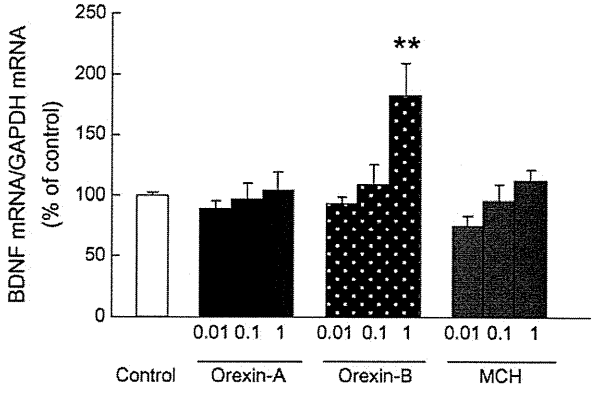

Fig. 4. Changes of mRNA expression of BDNF induced by incubation for 6 days with orexin-A, orexin-B and MCH (0.01, 0.1, and 1 μM). Data are presented as a percentage of the control. The values are mean ± S.E.M. from 11 RNA samples. $^{*}p < 0.05$, $^{**}p < 0.01$ vs. control group.

On the other hand, no change in the mRNA expression of NT-3 occurred on exposure to MCH (Fig. 3). The effects of these neuropeptides on BDNF mRNA expression were examined with the same RNA samples. Orexin-B at 1 μM significantly increased BDNF mRNA to 1.82-fold the control level, but its lower concentrations did not affect the mRNA expression of BDNF (Fig. 4). Neither orexin-A nor MCH changed the BDNF mRNA expression (Fig. 4).

In the present study, neuronal degeneration was not detected at 3 or 6 days after the application of neuropeptides (data not shown).

In the present study, the mRNA expression of NT-3 in primary cortical neuron cultures was markedly increased at 6 days after application of orexin-A and B, but not MCH. Moreover, only a high concentration of orexin-B significantly increased the expression of BDNF mRNA, while orexin-A and MCH did not. These findings suggest that orexins may be potent inducers of NT-3 in the cerebral cortex. Orexin and MCH are restrictedly present in the lateral hypothalamus and their neurons project to the cerebral cortex and hippocampus which contain their receptors. The radioimmunoreactive contents of orexins and MCH in the lateral hypothalamus have been shown to significantly increase in obese rodent models [19].

In the adult brain, especially in the cerebral cortex and hippocampus, BDNF and NT-3 act as neurotransmitter and neuromodulator in the central nervous system, and they act on TrkB and TrkC [5,25], respectively. Both BDNF and NT-3 have been implicated in the genesis of new synapses, which may be important for structural aspects of neuronal plasticity [18]. Neurotrophin expression in neurons is mainly regulated by neuronal depolarization [10,13], which may be an important mechanism in neuronal plasticity and may influence neuronal susceptibility to excitotoxicity. Chronic depolarization induced by K^+ (25 mM) in primary cultures of rat cerebellar neurons sustained a persistent increase of BDNF expression which is accompanied by a drastic decrease in NT-3 expression [7,10]. In contrast to the up-regulation of BDNF mRNA, the level of NT-3 mRNA does not change either after injection of kainic acid [1] or after kindled seizures [9]. Moreover, Rocamora et al. [21] have shown with an experimental model of limbic seizures that the dramatic increase of NGF and BDNF expression is accompanied by a fivefold decrease of NT-3 mRNA in dentate gyrus granule cells [21]. The reciprocal regulation of BDNF and NT-3 has also been observed in the dentate gyrus granule cells following cerebral ischemia [16,26]. Reduction of NT-3 mRNA in the hippocampal dentate gyrus was also demonstrated after long-term potentiation [6] and status epileptitus [3,20].

Several lines of evidence demonstrate the involvement of the glutamate nervous system in BDNF expression. Activation of the NMDA receptor, an ionotrophic glutamate receptor, increases BDNF gene expression in cortical neuron cultures [11]. Continuous culture exposure to non-toxic concentrations of NMDA resulted in a prolonged increase in BDNF mRNA expression in primary cultures of rat cerebellar granule neurons. In addition, AMPA also induced a concentration-dependent increase in BDNF mRNA and protein expression [17]. Moreover, an AMPA receptor potentiator (LY392098) was reported to increase BDNF mRNA levels, while it did not change in either NT-3 or NT-4 mRNA. Activation of both L-type Ca^{2+} channels and mitogen-activated protein (MAP) kinases contribute to AMPA receptor-mediated increases in BDNF mRNA [14]. AMPA antagonist CNQX, but not MK-801, suppresses kinase-induced increases in BDNF mRNA in hippocampal neuron cultures [32], while the activation of GABAergic transmission reduces the mRNA levels of BDNF [33]. These findings indicate that the neural depolarization induced by the activation of glutamate receptors increases BDNF expression.

These above-mentioned observations clearly demonstrate that NT-3 expression is suppressed by neuronal depolarization and, moreover, reciprocally regulated in contrast to BDNF expression in the brain. However, in the present experiment using primary cultured cortical neurons, orexin-A and B significantly up-regulated NT-3 mRNA expression, and orexin-B, to a lesser but significant extent, up-regulated the expression of BDNF mRNA. Although the mechanisms leading to reduced NT-3 mRNA expression induced by orexins has not yet been elucidated, orexins may be potent inducers of NT-3 in the cerebral cortex.

As above mentioned NT-3 as well as BDNF plays an important role in neurotransmission and neuronal plasticity in the brain, and its synthesis and release are regulated by neuronal depolarization. The present study demonstrated that orexins, but not MCH, increased the expression of NT-3 mRNA. It seems likely orexin might act on some neurons which was different from neurons containing MCH receptors. Orexin is well known as orexigenic neuropeptide in the hypothalamus and is regulated by hunger status. Orexin released in response to the peripheral metabolic signals may increase NT-3 mRNA in the cerebral cortex, resulting in the modulation of neuronal transmission in the cerebral cortex.

The findings in the present study indicate that these neuropeptides involved in energy regulation may regulate the expressions of NT-3 and BDNF in the cerebral cortex, indicating that these neuropeptides can regulate the activity of the cerebral cortex via changes in neuronal plasticity. These findings offer information for understanding the functional significance of NT-3 in obese animals and a new insight into the bidirectional interaction between energy regulation and higher functions of the limbic system, such as learning/memory and emotion.

References

[1] M. Ballarin, P. Ernfors, N. Lindefors, H. Persson, Hippocampal damage and kainic acid injection induce a rapid increase in mRNA for BDNF and NGF in the rat brain, Exp. Neurol. 114 (1991) 35–43.
[2] M. Barbacid, The Trk family of neurotrophin receptors, J. Neurobiol. 25 (1994) 1386–1403.
[3] J. Bengzon, Z. Kokaia, P. Ernfors, M. Kokaia, G. Leanza, O.G. Nilsson, H. Persson, O. Lindvall, Regulation of neurotrophin and trkA, trkB and trkC tyrosine kinase receptor messenger RNA expression in kindling, Neuroscience 53 (1993) 433–446.
[4] S.L. Borgland, S.A. Taha, F. Sarti, H.L. Fields, A. Bonci, Orexin A in the VTA is critical for the induction of synaptic plasticity and behavioral sensitization to cocaine, Neuron 49 (2006) 589–610.
[5] M. Bothwell, Functional interactions of neurotrophins and neurotrophin receptors, Annu. Rev. Neurosci. 18 (1995) 223–253.
[6] E. Castrén, M. Pitkanen, J. Sirvio, A. Parsadanian, D. Lindholm, H. Thoenen, P.J. Riekkinen, The induction of LTP increases BDNF and NGF mRNA but decreases NT-3 mRNA in the dentate gyrus, Neuroreport 4 (1993) 895–898.
[7] D.F. Condorelli, P. Dell'Albani, T. Timmusk, G. Mudo, N. Belluardo, Differential regulation of BDNF and NT-3 mRNA levels in primary cultures of rat cerebellar neurons, Neurochem. Int. 32 (1998) 87–91.

[8] J.C. Elliott, J.A. Harrold, P. Brodin, K. Enquist, A. Bäckman, M. Byström, K. Lindgren, P. King, G. Williams, Increases in melanin-concentrating hormone and MCH receptor levels in the hypothalamus of dietary-obese rats, Mol. Brain Res. 128 (2004) 150–159.
[9] P. Ernfors, J. Bengzon, Z. Kokaia, H. Persson, O. Lindvall, Increased levels of messenger RNAs for neurotrophic factors in the brain during kindling epileptogenesis, Neuron 7 (1991) 165–176.
[10] M. Favaron, R.M. Manev, J.M. Rimland, P. Candeo, M. Beccaro, H. Manev, NMDA-stimulated expression of BDNF mRNA in cultured cerebellar granule neurons, Neuroreport 4 (1993) 1171–1174.
[11] A. Ghosh, J. Carnahan, M.E. Greenberg, Requirement for BDNF in activity-dependent survival of cortical neurons, Science 263 (1994) 1618–1623.
[12] T.S. Kilduff, L. de Lecea, Mapping of the mRNAs for the hypocretin/orexin and melanin-concentrating hormone receptors: networks of overlapping peptide systems, J. Comp. Neurol. 435 (2001) 1–5.
[13] J.C. Lauterborn, G. Lynch, P. Vanderklish, A. Arai, C.M. Gall, Positive modulation of AMPA receptors increases neurotrophin expression by hippocampal and cortical neurons, J. Neurosci. 20 (2000) 8–21.
[14] B. Legutko, X. Li, P. Skolnick, Regulation of BDNF expression in primary neuron culture by LY39098, a novel AMPA receptor potentiator, Neuropharmacology 40 (2001) 1019-1-27.
[15] G.R. Lewin, Y.A. Barde, Physiology of the neurotrophins, Annu. Rev. Neurosci. 19 (1996) 289–317.
[16] O. Lindvall, P. Ernfors, J. Bengzon, Z. Kokaia, M.L. Smith, B.K. Siesjo, H. Persson, Differential regulation of mRNAs for nerve growth factor, brain-derived neurotrophic factor, and neurotrophin 3 in the adult rat brain following cerebral ischemia and hypoglycemic coma, Proc. Natl. Acad. Sci. U.S.A. 89 (1992) 648–652.
[17] B.P. Lockhart, M. Rodriguez, S. Mourlevat, P. Peron, S. Catesson, N. Villain, J.P. Galizzi, J.-A. Boutin, P. Lestage, S18986: a positive modulator of AMPA-receptors enhances (S)-AMPA-mediated BDNF mRNA and protein expression in rat primary cortical neuronal cultures, Eur. J. Pharmacol. 561 (2007) 23–31.
[18] B. Lu, A. Chow, Neurotrophins and hippocampal synaptic transmission and plasticity, J. Neurosci. Res. 58 (1999) 76–87.
[19] M.S. Mondal, M. Nakazato, S. Matsukura, Characterization of orexins (hypocretins) and melanin-concentrating hormone in genetically obese mice, Regul. Pept. 104 (2002) 21–25.
[20] G. Mudó, X.H. Jiang, T. Timmusk, M. Bindoni, N. Belluardo, Change in neurotrophins and their receptor mRNAs in the rat forebrain after status epilepticus induced by pilocarpine, Epilepsia 37 (1996) 198–207.
[21] N. Rocamora, J.M. Palacios, G. Mengod, Limbic seizures induce a differential regulation of the expression of nerve growth factor, brain-derived neurotrophic factor and neurotrophin-3, in the rat hippocampus, Brain Res. Mol. Brain Res. 13 (1992) 27–33.
[22] A.F. Schinder, M.M. Poo, The neurotrophin hypothesis for synaptic plasticity, Trends Neurosci. 23 (2000) 639–645.
[23] M.W. Schwartz, S.C. Woods, D. Porte Jr., R.J. Seeley, D.G. Baskin, Central nervous system control of food intake, Nature 404 (2000) 661–671.
[24] O. Selbach, N. Doreulee, C. Bohla, K.S. Eriksson, O.A. Sergeeva, W. Poelchen, R.E. Brown, H.L. Haas, Orexins/hypocretins cause sharp wave- and theta-related synaptic plasticity in the hippocampus via glutamatergic, gabaergic, noradrenergic, and cholinergic signaling, Neuroscience 127 (2004) 519–528.
[25] D. Sopper, E. Escandon, J. Maragos, D.S. Middlemas, S.W. Reid, J. Blair, L.E. Burton, B.R. Stanton, D.R. Kaplan, T. Hunter, K. Nikolics, L.F. Parada, The neurotrophic factors brain-derived neurotrophic factor and neurotrophine-3 are ligands for the TrkB tyrosine kinase receptor, Cell 65 (1991) 895–903.
[26] A. Takeda, H. Onodera, Y. Yamasaki, K. Furukawa, K. Kogure, M. Obinata, S. Shibahara, Decreased expression of neurotrophin-3 mRNA in the rat hippocampus following transient forebrain ischemia, Brain Res. 569 (1992) 177–180.
[27] H. Thoenen, Neurotrophins and activity-dependent plasticity, Prog. Brain Res. 128 (2000) 183–191.
[28] M. van den Top, K. Lee, A.D. Whyment, A.M. Blanks, D. Spanswick, Orexigen-sensitive NPY/AgRP pacemaker neurons in the hypothalamic arcuate nucleus, Nat. Neurosci. 7 (2004) 493–494.
[29] M. Varas, M. Pérez, O. Ramírez, S.R. de Barioglio, Melanin concentrating hormone increase hippocampal synaptic transmission in the rat, Peptides 23 (2002) 151–155.
[30] M.M. Yaghoobi, S.J. Mowla, Differential gene expression pattern of neurotrophins and their receptors during neuronal differentiation of rat bone marrow stromal cells, Neurosci. Lett. 397 (2006) 149–154.
[31] N. Yamada, G. Katsuura, I. Tatsuno, T. Asaki, S. Kawahara, K. Ebihara, Y. Saito, K. Nakao, Orexin decreases the mRNA expressions of NMDA and AMPA receptor subunits in rat primary neuron cultures, Peptides, in press.
[32] F. Zafra, B. Hengerer, J. Leibrock, H. Thoenen, D. Lindholm, Activity dependent regulation of BDNF and NGF mRNAs in the rat hippocampus is mediated by non-NMDA glutamate receptors, EMBO J. 9 (1990) 3545–3550.
[33] F. Zafra, E. Castrén, H. Thoenen, D. Lindholm, Interplay between glutamate and gamma-aminobutyric acid transmitter systems in the physiological regulation of brain-derived neurotrophic factor and nerve growth factor synthesis in hippocampal neurons, Proc. Natl. Acad. Sci. U.S.A. 88 (1991) 10037–10041.

Am J Physiol Endocrinol Metab 297: E802–E811, 2009.
First published July 14, 2009; doi:10.1152/ajpendo.00205.2009.

A mouse model of ghrelinoma exhibited activated growth hormone-insulin-like growth factor I axis and glucose intolerance

Hiroshi Iwakura,[1] Hiroyuki Ariyasu,[1] Yushu Li,[1] Naotetsu Kanamoto,[2] Mika Bando,[1] Go Yamada,[2] Hiroshi Hosoda,[4] Kiminori Hosoda,[2] Akira Shimatsu,[3] Kazuwa Nakao,[2] Kenji Kangawa,[1,4] and Takashi Akamizu[1]

[1]*Ghrelin Research Project, Translational Research Center, Kyoto University Hospital, Kyoto University Graduate School of Medicine;* [2]*Department of Medicine and Clinical Science, Endocrinology, and Metabolism, Kyoto University Graduate School of Medicine;* [3]*Clinical Research Institute for Endocrine Metabolic Diseases, National Hospital Organization, Kyoto Medical Center, Kyoto; and* [4]*Department of Biochemistry, National Cardiovascular Center Research Institute, Osaka, Japan*

Submitted 27 March 2009; accepted in final form 13 July 2009

Iwakura H, Ariyasu H, Li Y, Kanamoto N, Bando M, Yamada G, Hosoda H, Hosoda K, Shimatsu A, Nakao K, Kangawa K, Akamizu T. A mouse model of ghrelinoma exhibited activated growth hormone-insulin-like growth factor I axis and glucose intolerance. *Am J Physiol Endocrinol Metab* 297: E802–E811, 2009. First published July 14, 2009; doi:10.1152/ajpendo.00205.2009.—Ghrelin is a stomach-derived peptide that has growth hormone-stimulating and orexigenic activities. Although there have been several reports of ghrelinoma cases, only a few cases have elevated circulating ghrelin levels, hampering the investigation of pathophysiological features of ghrelinoma and chronic effects of ghrelin excess. Furthermore, standard transgenic technique has resulted in desacyl ghrelin production only because of the limited tissue expression of ghrelin *O*-acyltransferase, which mediates acylation of ghrelin. Accordingly, we attempted to create ghrelin promoter SV40 T-antigen transgenic (GP-Tag Tg) mice, in which ghrelin-producing cells continued to proliferate and finally developed into ghrelinoma. Adult GP-Tag Tg mice showed elevated plasma ghrelin levels with preserved physiological regulation. Adult GP-Tag Tg mice with increased plasma ghrelin levels exhibited elevated IGF-I levels despite poor nutrition. Although basal growth hormone levels were not changed, those after growth hormone-releasing hormone injection tended to be higher. These results indicate that chronic elevation of ghrelin activates GH-IGF-I axis. In addition, GP-Tag Tg mice demonstrated glucose intolerance. Insulin secretion by glucose tolerance tests was significantly attenuated in GP-Tag Tg, whereas insulin sensitivity determined by insulin tolerance tests was preserved, indicating that chronic elevation of ghrelin suppresses insulin secretion and leads to glucose intorelance. Thus, we successfully generated a Tg model of ghrelinoma, which is a good tool to investigate chronic effects of ghrelin excess. Moreover, their characteristic features could be a hint on ghrelinoma.

ghrelin; glucose metabolism

GHRELIN is a stomach-derived 28-amino acid (AA) peptide hormone with octanoyl modification of third Ser residue, which is essential for its binding to growth hormone (GH) secretagogue receptor (GHS-R) (20). There have been several reports regarding ghrelin-producing tumors (9, 17, 36, 37). As far as we know, only two cases have elevated plasma ghrelin level (9, 36). However, the ghrelin-producing cells in the stomach, known as X/A-like cells, account for about 20% of the endocrine cell population in the oxyntic glands (10). It may be reasonable to estimate that far more ghrelinoma cases have been overlooked and diagnosed as nonfunctioning tumors. Hormone-producing tumors demonstrate their characteristic symptoms by chronic effects of each hormone, which may be a key symptom to making a correct diagnosis. Conversely, the characteristic symptom often tells us the chronic effects of each responsible hormone. Acute effects of ghrelin have been studied extensively by many researchers, and a wide variety of acute effects of ghrelin have been discovered, such as the regulation of growth hormone (GH) release, food intake, gastric acid secretion, gastric motility, blood pressure, and cardiac output (23, 25, 26, 31, 33, 34). However, chronic effects of ghrelin have not been fully understood.

To understand the chronic effects of ghrelin, genetically engineered mouse models would be useful. Several groups, including ours, have developed transgenic animals in which ghrelin transgenes are driven by several different promoters (2, 4, 18, 29, 38, 41). All of these animals except for one line created by Reed et al. (29) using the neuron-specific enolase (NSE) promoter and another line recently reported by Bewick et al. (5) using the bacterial artificial chromosome produced only desacyl ghrelin rather than acylated ghrelin. Until the recent identification of ghrelin *O*-acyltransferase (GOAT), which mediates ghrelin octanoylation (40), it had been unclear how acylation of ghrelin takes place. GOAT is expressed mainly in stomach and intestine, and a small amount of GOAT is also present in pancreas (12). This limited expression area of GOAT made it impossible to create ghrelin-overproducing transgenic animals by standard procedures. When we started this study, GOAT had not yet been identified. Accordingly, we choose an approach in which an increase in the number of ghrelin-producing cells in mice would result in increased levels of circulating ghrelin. By taking this approach, we successfully obtained ghrelin promoter-SV40 T-antigen transgenic (GP-Tag Tg) mice. In these mice, ghrelin concentration elevates with age in concordance with the proliferation of ghrelin cells. The aim of this study was to elucidate the pathophysiological features of ghrelinoma and the chronic effects of ghrelin elevation.

MATERIALS AND METHODS

Animals. Two types of fusion genes comprising the 5′-flanking region of human ghrelin gene (4,085 or 1,479 bp) (19) and SV40 T-antigen were designed (Fig. 1*A*). The purified fragments (10 μg/ml) were microinjected into the pronucleus of fertilized C57/B6 mouse (SLC, Shizuoka, Japan) eggs. The viable eggs were transferred into the oviducts of pseudopregnant female ICR mice (SLC) by using standard techniques. Transgenic founder mice were identified by

Address for reprint requests and other correspondence: H. Iwakura, Ghrelin Research Project, Translational Research Center, Kyoto University Hospital, 54 Shogoin Kawahara-cho, Sakyo-ku, Kyoto 606-8507, Japan (e-mail: hiwaku@kuhp.kyoto-u.ac.jp).

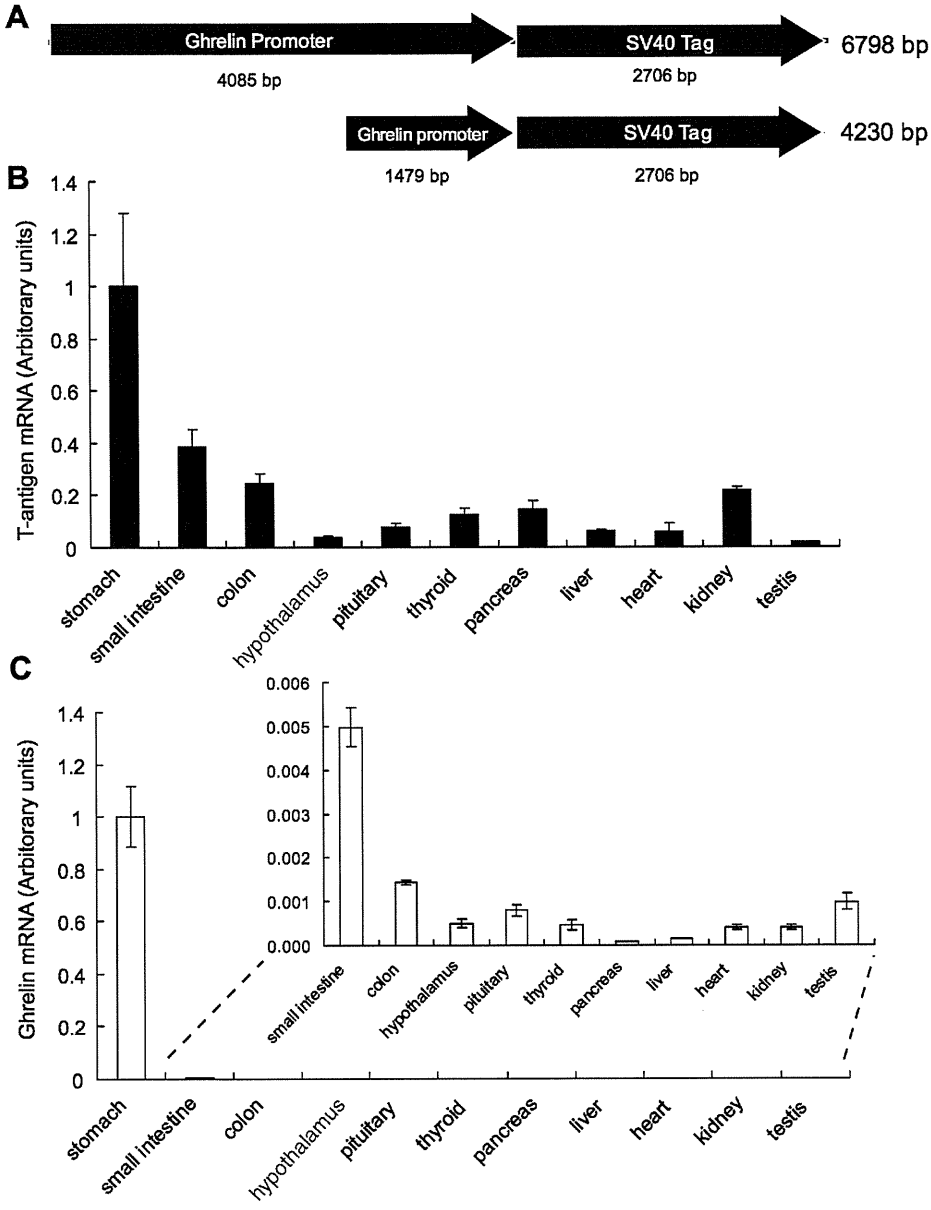

Fig. 1. Constructs of ghrelin promoter-SV40 T-antigen transgenic (GP-Tag Tg) mice and the expression levels of SV40 T-antigen mRNA in various tissues. *A*: 2 types of fusion genes comprising 5′-flanking region of human ghrelin gene (4,085 or 1,479 bp) and SV40 Tag were designed. *B*: the expression levels of SV40 T-antigen mRNA in various tissues of GP-Tag Tg mice at 6 wk of age (n = 8). SV40 T-antigen mRNA was most abundant in the stomachs of GP-Tag Tg mice. *C*: the expression levels of ghrelin mRNA in various tissues of nontransgenic littermates at 6 wk of age (n = 4).

Southern blot analysis of tail DNAs. Transgenic mice were used as heterozygotes. Animals were maintained on standard rodent food (CE-2, 352 kcal/100 g; Japan CLEA, Tokyo, Japan) on a 12:12-h light-dark cycle unless otherwise indicated. All experimental procedures were approved by the Kyoto University Graduate School of Medicine Committee on Animal Research.

RT-PCR and real-time quantitative RT-PCR. Total RNA was extracted using a Sepasol RNA kit (Nacalai Tesque, Kyoto, Japan). Reverse transcription was performed with a high-capacity cDNA reverse transcription kit (Applied Biosystems, Foster City, CA). RT-PCR was carried out with a GeneAmp 9700 using primers in Table 1 with AmpliTaq Gold PCR master mix (Applied Biosystems). Real-time quantitative PCR was performed using an ABI PRISM 7500 Sequence Detection System (Applied Biosystems) with primers and TaqMan probes or with Power SybrGreen (presented in Table 1). The mRNA expression in each gene was normalized to levels of 18S ribosomal RNA.

Immunohistochemistry. Formalin-fixed, paraffin-embedded tissue sections were immunostained using the avidin-biotin peroxidase complex method (Vectastain "ABC" Elite kit; Vector Laboratories, Burlingame, CA), as described previously (18). Sections were incubated with anti-COOH-terminal ghrelin (AA 13-28) (1:2,000 at final dilution), anti-NH_2-terminal ghrelin (14) that recognizes the n-octanoylated portion of ghrelin (AA 1-11) (1:5,000), anti-glucagon (1:500; DAKO, Glostrup, Denmark), anti-somatostatin (1:500; DAKO), anti-gastrin (1:500; DAKO), and anti-GH (1:500; DAKO). The cell number of ghrelin-immunopositive cells was analyzed by WinRoof visual analysis software (Mitani, Fukui, Japan).

Measurements of plasma and tissue ghrelin concentrations. Collection of plasma samples was performed as reported previously (18). Plasma ghrelin and desacyl ghrelin concentrations were determined using two separate ELISA kits, an active ghrelin ELISA kit that recognizes n-octanoylated ghrelin and a desacyl ghrelin ELISA kit (both from Mitsubishi Kagaku Iatron, Tokyo, Japan) (1). Tissue ghrelin concentration was determined by radioimmunoassay (RIA) using anti-ghrelin (AA 13-28) antiserum (C-RIA) and anti-ghrelin (AA 1-11) antiserum (N-RIA), as described previously (18).

Western blot. Stomachs were boiled for 5 min in the 10-fold vol/wt of water. Acetic acid was added to each solution so that the final concentration was adjusted to 1 M, and the tissues were homogenized.

Table 1. *PCR primers and TaqMan probes*

Gene	Primer Sequence
Ghrelin	
Sense	5′-GCATGCTCTGGATGGACATG-3′
Antisense	5′-TGGTGGCTTCTTGGATTCCT-3′
TaqMan probe	5′-AGCCCAGAGCACCAGAAAGCCCA-3′
NPY	
Sense	5′-TCCGCTCTGCGACACTACAT-3′
Antisense	5′-GGAAGGGTCTTCAAGCCTTGT-3′
TaqMan probe	5′-CAAGGGCTGGATCTCTTGCCATATCTCTG-3′
AgRP	
Sense	5′-GCTCCACTGAAGGGCATCA-3′
Antisense	5′-TAGCACCTCCGCCAAAGCT-3′
TaqMan probe	5′-TTCCCAGGTCTAAGTCTGAATGGCCTCA-3′
GHRH	
Sense	5′-AGGATGCAGCGACACGTAGA-3′
Antisense	5′-TCTCCCCTTGCTTGTTCATGA-3′
TaqMan probe	5′-CCACCAACTACAGGAAACTCCTGAGCCA-3′
Somatostatin	
Sense	5′-AGCTGAGCAGGACGAGATGAG-3′
Antisense	5′-ACAGGATGTGAATGTCTTCCAGTT-3′
TaqMan probe	5′-CGAACCCAGCAATGGCACCCC-3′
GHS-R	
Sense	5′-CACCAACCTCTACCTATCCAGCAT-3′
Antisense	5′-CTGACAAACTGGAAGAGTTTGCA-3′
TaqMan probe	5′-TCCGATCTGCTCATCTTCCTGTGCATG-3′
GH	
Sense	5′-AAGAGTTCGAGCGTGCCTACA-3′
Antisense	5′-GAAGCAATTCCATGTCGGTTC-3′
TaqMan probe	5′-CCATTCAGAATGCCCAGGCTGCTTTC-3′
GHRH-R	
Sense	5′-GCCCTTGGAACTGTTAACCA-3′
Antisense	5′-GCAACCAGGATGGCAATAGC-3′
TaqMan probe	5′-AGCATCTCCATTGTAGCCCTCTGCGTG-3′
SV40 Tag	
Sense	5′-AAACACTGCAGGCCAGATTT-3′
Antisense with power SYBR Green	5′-AAATGAGCCTTGGGACTGTG-3′
PC1/3	
Sense	5′-AGTGGAAAAGATGGTGAATG-3′
Antisense	5′-CTCCTCATTTAGGATGTCCA-3′

NPY, neuropeptide Y; AgRP, agouti-related protein; GHRH, growth hormone (GH)-releasing hormone; GHS-R, GH secretagogue receptor; GHRH-R, GHRH receptor; PC1/3, prohormone convertase 1/3.

The supernatant was loaded onto a Sep-Pak C18 cartridge (Waters, Milford, MA) preequilibrated with 0.9% NaCl after centrifugation. The cartridge was washed with 2.5 ml of 5% CH_3CN-0.1% trifluoroacetic acid and eluted with 2.5 ml 60% CH_3CN-0.1% trifluoroacetic acid. The eluate was evaporated, lyophilized, and dissolved in Novex Tricine SDS Sample Buffer (Invitrogen, Carlsbad, CA). After being heated at 85°C for 2 min, 20 mg of samples of initial weight were subjected to tricine-SDS PAGE and electroblotted to polyvinylidene fluoride membranes (Invitrogen). Transferred membranes were blocked with Immunoblock (Dainippon Seiyaku, Osaka, Japan) and then incubated with anti-COOH-terminal ghrelin antibody (1:5,000). After being washed with PBS-0.1% Tween-20, membranes were reacted with secondary antibodies and developed with ECL plus (GE Healthcare, Buckinghamshire, UK) as instructed by the manufacturer. The signal on the blot was detected with Lumino-Image Analyzer LAS-3000 mini system (Fuji Photo Film, Tokyo, Japan).

Measurement of food intake. Mice were housed individually with continuous access to chow and water. Food intakes were measured by subtracting the remaining weight of the chow from that originally presented. As for measuring the food intake by ghrelin, ad libitum-fed mice were injected with ghrelin (120 or 360 μg/kg) or saline subcutaneously. Food intakes were measured for 2 h after injection.

Measurements of lean body mass, fat mass, and bone mass. Mice were anesthetized with pentobarbital sodium. Lean body mass, fat mass, and bone mass of mice were measured by an animal computed tomography system (Latheta LTC-100; Aloka, Tokyo, Japan).

Measurements of hormones and blood glucose levels. Serum GH levels were determined by a rat GH EIA kit (SPI Bio, Massy Cedex, France). Serum insulin-like growth factor I (IGF-I) levels were measured using a mouse IGF-I immunoassay kit (R & D Systems, Minneapolis, MN). Blood glucose levels were determined by glucose oxidase method using Glutest Sensor Neo (Sanwa Kagaku, Kyoto, Japan). Measurement of serum insulin concentrations was performed by ELISA using an ultrasensitive rat insulin kit (Morinaga, Yokohama, Japan).

GH-provocative test. GH-provocative test was carried out as described previously (16). Serum samples were collected at 15 min after subcutaneous injection of 180 μg/kg of GH-releasing hormone (GHRH) or 120 μg/kg of ghrelin. We choose these doses according to the results of our previous study (16).

Glucose and insulin tolerance tests. For the glucose tolerance test, after overnight fast, the mice were injected with 1.5 g/kg glucose intraperitoneally. For the insulin tolerance test, after a 4-h fast, mice were injected with 1.0 mU/g human regular insulin (Novolin R; Novo Nordisk, Bagsvaerd, Denmark) intraperitoneally. Blood was sampled from the tail vein before and 30, 60, 90, and 120 min after the injection.

Insulin release. After overnight fast, the mice were injected with 3.0 g/kg glucose intraperitoneally. Blood was sampled from the retroorbital vein at 2 and 30 min after the injection using a glass tube.

Statistical analysis. All values were expressed as means ± SE. The statistical significance of the differences in mean values was assessed by repeated-measures ANOVA or Student's *t*-test. The statistical difference in the changes of plasma ghrelin levels by feeding were assessed by paired *t*-test. Pearson's correlation coefficient analysis and simple regression were used to assess the relations between plasma ghrelin level and body weight. Difference of correlation coefficients of the regression lines obtained from GP-Tag Tg mice and nontransgenic littermates was determined by testing the *t* value.

RESULTS

Generation of GP-Tag Tg mice. By injecting transgenes into 846 eggs, we obtained 11 lines of GP (4.85) Tag Tg mouse. We succeeded in breeding three of these lines (1-5, 3-1, and 4-3). Among these three lines, mice of the 3-1 line developed gastric tumor and showed elevated plasma ghrelin levels, as described below. Mice of the 1-5 line showed very aggressive tumor development and died at ~13 wk of age because of thyroid, pancreatic, and gastric tumors. Mice of the 4-3 line showed very slow tumor development. The proliferation of ghrelin cells was

Fig. 2. Pathological findings and tissue ghrelin concentrations of stomachs in GP-Tag Tg mice. *A–C*: macro findings of stomachs in GP-Tag Tg mice (*A*: arrow, dotted area; *B*: Tg) and nontransgenic littermates (non; *B*) at 12 wk of age. Stomach walls of GP-Tag Tg mice were hypertrophic. *C*: immunohistochemical analysis of ghrelin peptide expression in tissue sections of stomachs of GP-Tag Tg mice (Tg) and nontransgenic littermates (non) using anti-COOH-terminal and anti-NH_2-terminal ghrelin antibodies. *D*: the cell number of ghrelin-immunopositive cells in Tg and non littermates. *E*: the mRNA levels of ghrelin in 12-wk-old male Tg mice and non littermates; $n = 5$, $^{**}P < 0.01$ compared with nontransgenic littermates. *F* and *G*: tissue concentration per milligram (*F*) and per stomach (*G*) of ghrelin peptide in 12-wk-old male Tg mice (black bars) and non littermates (open bars); $n = 6$, $^{**}P < 0.01$ compared with non littermates. C-RIA, total ghrelin (ghrelin and desacyl ghrelin); N-RIA, ghrelin. *H*: Western blot analysis of stomach samples of Tg and non littermates using anti COOH-terminal ghrelin antibody. *I*: RT-PCR analysis of prohormone convertase 1/3 (PC1/3) mRNA expression in the stomach of Tg.

modest even at 50 wk of age in the 4-3 line. Accordingly, we analyzed mainly GP-Tag Tg mice of the 3-1 line.

We could not get a transgene-positive mouse of GP (1479) Tag Tg mouse by injecting transgenes into 631 eggs.

The expression levels of SV40-Tag mRNA among various tissues. We first examined the expression levels of SV40-Tag mRNA in various tissues of GP-Tag Tg mice, including stomach, small intestine, colon, hypothalamus, pituitary, thyroid,

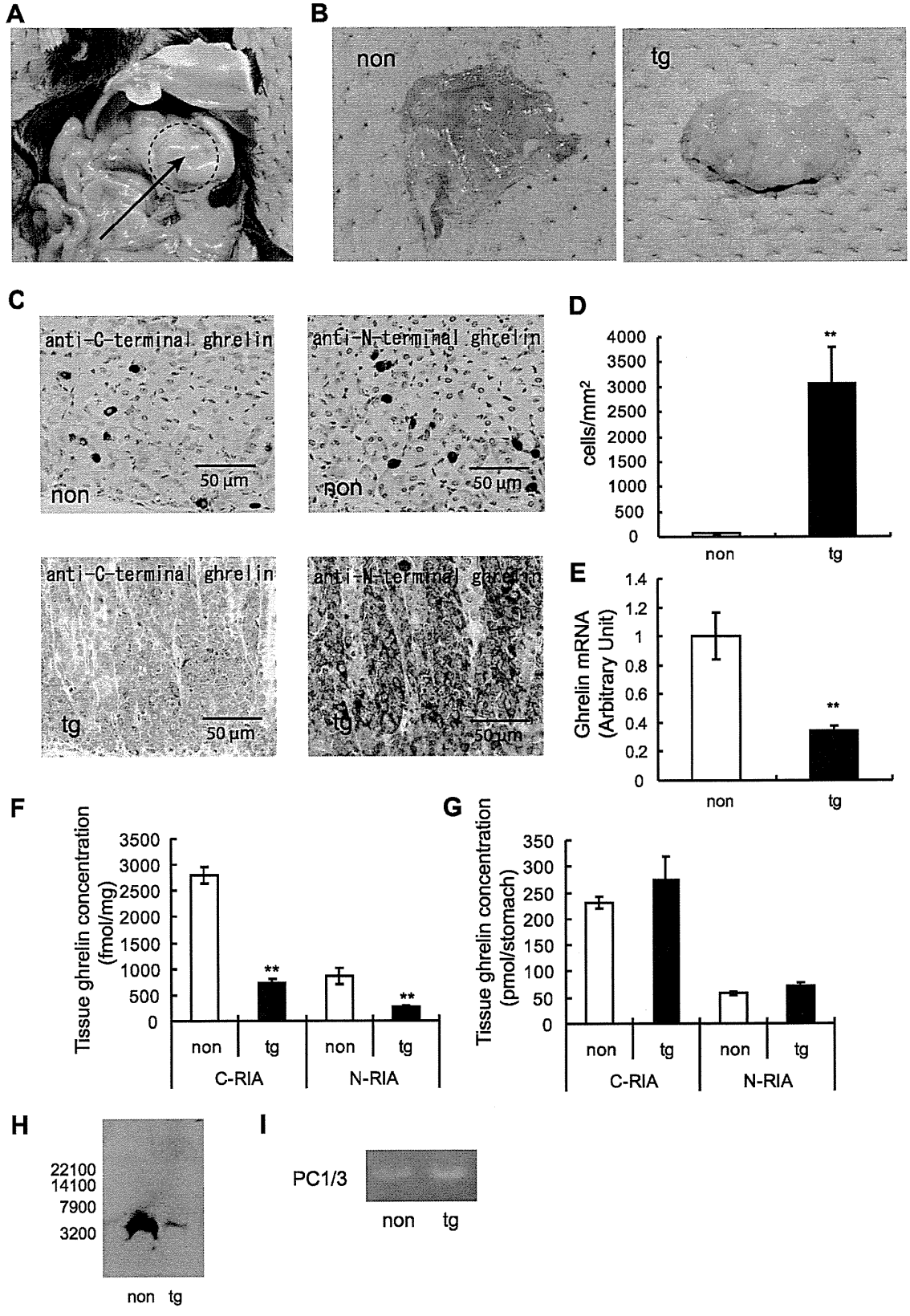

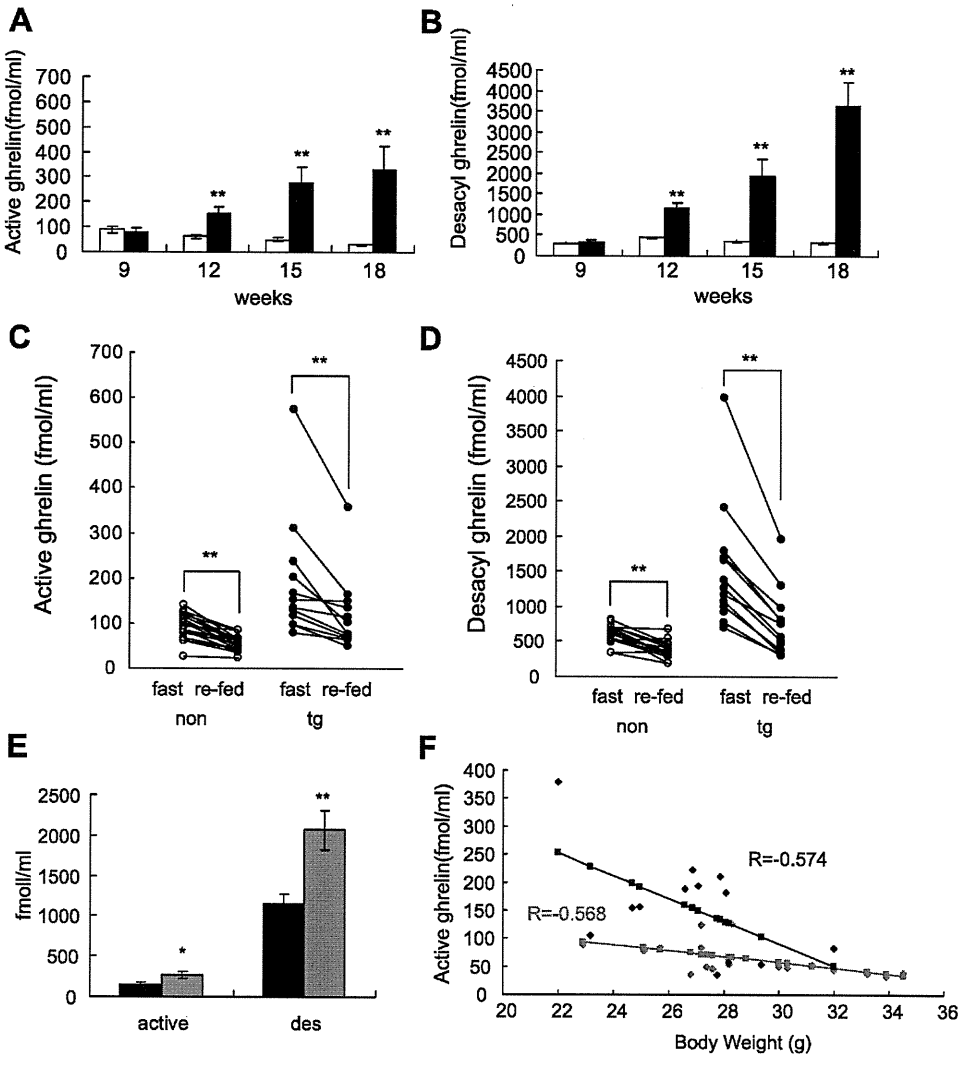

Fig. 3. Plasma ghrelin and desacyl ghrelin levels in GP-Tag Tg mice. *A* and *B*: plasma ghrelin (*A*) and desacyl ghrelin (*B*) levels in male GP-Tag Tg mice (black bars) and nontransgenic littermates (open bars); $n = 3$–17. $^{**}P < 0.01$ compared with non littermates. *C* and *D*: plasma ghrelin (*C*) and desacyl ghrelin (*D*) levels after overnight fasting (fast) and after refeeding (refed) in 15-wk-old male Tg and non mice. $^{**}P < 0.01$; $n = 12$–18. *E*: plasma ghrelin (active) and desacyl ghrelin (des) levels in 12-wk-old male (black bars) and female (gray bars) GP-Tag Tg mice; $n = 7$–13, $^{*}P < 0.05$, $^{**}P < 0.01$ compared with male GP-Tag Tg mice. *F*: plasma ghrelin levels were correlated with body weights in 12-wk-old male GP-Tag Tg mice (black bars; $r = -0.574$, $P < 0.01$) and in nontransgenic littermates (gray bars; $r = -0.568$, $P < 0.05$). The regression coefficient of the regression line of GP-Tag Tg mice was bigger than that of nontransgenic littermates ($t = 2.08$, $P < 0.05$).

pancreas, liver, heart, kidney, and testis (Fig. 1*B*). The highest expression levels were observed in stomach, and the second-highest levels were observed in small intestine. The expression pattern of SV40-Tag mRNA was almost similar to that of ghrelin (Fig. 1*C*).

Pathological feature and tissue ghrelin concentration of stomach of GP-Tag Tg mice. Stomach walls of GP-Tag Tg mice became hypertrophic with age (Fig. 2, *A* and *B*). Immunohistochemical analysis by both anti-COOH-terminal and anti-NH_2-terminal ghrelin antibodies revealed hyperplasia of ghrelin-immunopositive cells (Fig. 2, *C* and *D*), although the staining in GP-Tag Tg mice was paler than that in nontransgenic littermates (Fig. 2*C*). These hyperproliferating cells were not immunostained with anti-glucagon, somatostatin, or gastrin antibodies (data not shown).

The mRNA levels of ghrelin in the stomachs of 12-wk-old male GP-Tag Tg mice were significantly lower than those of nontransgenic littermates ($P < 0.01$, $n = 6$; Fig. 2*E*). Consistent with this observation, tissue concentrations of ghrelin (N-RIA; fmol/mg tissue) and total ghrelin (desacyl ghrelin plus ghrelin) (C-RIA) of 12-wk-old male GP-Tag Tg mice were significantly lower than those of nontransgenic littermates ($P < 0.01$, $n = 6$; Fig. 2*F*). However, since the weights of the stomach of GP-Tag Tg mice were significantly higher than controls (non-Tg vs. Tg, 83.4 vs. 362.0 mg, $P < 0.01$) due to the hypertrophy of the stomach wall, the tissue ghrelin concentration per whole stomach tended to be higher in GP-Tag Tg mice [not significant (NS), $n = 6$; Fig. 2*G*]. The size of ghrelin content of GP-Tag Tg mice was similar to that of nontransgenic littermates when analyzed by tricine-SDS PAGE and Western blot analysis (Fig. 2*H*), indicating that processing of preproghrelin to ghrelin occurred in hyperproliferaing ghrelin cells in GP-Tag Tg mice. The mRNA of prohormone convertase 1/3, which processes preproghrelin to ghrelin, was detected in the stomachs of GP-Tag Tg mice (Fig. 2*I*).

Plasma ghrelin levels of GP-Tag Tg mice. Plasma ghrelin and desacyl ghrelin levels of GP-Tag Tg mice were almost equal to those of nontransgenic littermates at 9 wk of age and then increased with age ($n = 3$–17; Fig. 3, *A* and *B*), with some variations in the levels among animals.

We next examined whether physiological regulation of ghrelin secretion is preserved in GP-Tag Tg mice. Plasma ghrelin and desacyl ghrelin levels of GP-Tag Tg mice were increased by fasting and decreased by refeeding $P < 0.01$, ($n = 7$–13; Fig. 3, *C* and *D*). Plasma ghrelin and desacyl ghrelin levels of female GP-Tag Tg mice were significantly higher than those of

male GP-Tag Tg mice at 12 wk of age (Fig. 3*E*). Plasma ghrelin levels of 12-wk-old male GP-Tag Tg mice correlated to body weight ($r = 0.574$, $P < 0.05$, $n = 13$; Fig. 3*F*). The regression coefficient of the regression line of GP-Tag Tg mice was bigger than that of nontransgenic littermates ($t = 2.08$, $P < 0.05$) These results indicate that regulation of plasma ghrelin and desacyl ghrelin levels of GP-Tag Tg mice were preserved, at least with regard to feeding status, body weight, and sex difference.

Body weights, body composition, and food intake of GP-Tag Tg mice. There was no difference in body weights between male GP-Tag Tg mice and controls until 12 wk of age ($n = 22–34$; Fig. 4*A*). After 13 wk of age, the body weights of the male GP-Tag Tg mice were significantly lower than those of nontransgenic littermates concomitantly with the decrease in the food intakes of male GP-Tag Tg mice after 11 wk of age (Fig. 4, *A* and *B*). When the body compositions were examined by computed tomography scan, fat masses were significantly reduced in 15-wk-old male GP-Tag Tg mice ($P < 0.05$, $n = 7–9$; Fig. 4*C*), whereas lean body masses and body lengths were not changed (NS, $n = 7–9$; Fig. 4, *D* and *E*). We also examined hypothalamic mRNA levels of neuropeptide Y (NPY), agouti-related protein (AgRP), and GHS-R in 12-wk-old male GP-Tag Tg mice. No significant changes were observed in these mRNA levels (NS, $n = 7$; Fig. 4*F*). When 15-wk-old male GP-Tag Tg mice were injected with ghrelin, the food intake was stimulated to the same extent as in controls (NS, $n = 10–18$; Fig. 4*G*). Plasma leptin levels of 15-wk-old male GP-Tag Tg mice were significantly lower than controls ($P < 0.05$, $n = 6$; Fig. 4*H*).

GH-IGF-I axis in GP-Tag Tg mice. Serum IGF-I levels of 12- and 15-wk-old male GP-Tag Tg mice were significantly higher than those of nontransgenic littermates ($P < 0.05$, $n = 7–8$, and $P < 0.05$, $n = 6–7$, respectively; Fig. 5*A*). Although basal serum GH levels of 15-wk-old male GP-Tag Tg mice were not significantly different from controls, serum GH levels after GHRH injection tended to be high ($P = 0.077$, $n = 8–13$), which was not observed after ghrelin injection (Fig. 5*B*). We then investigated the effects of chronic ghrelin elevation on hypothalamic and pituitary mRNA levels of components involved in GH regulation. There were no differences in hypothalamic mRNA levels of GHRH and somatostatin or in pituitary mRNA levels of GH and GHRH receptor (GHRH-R) between 15-wk-old male GP-Tag Tg mice and their littermates

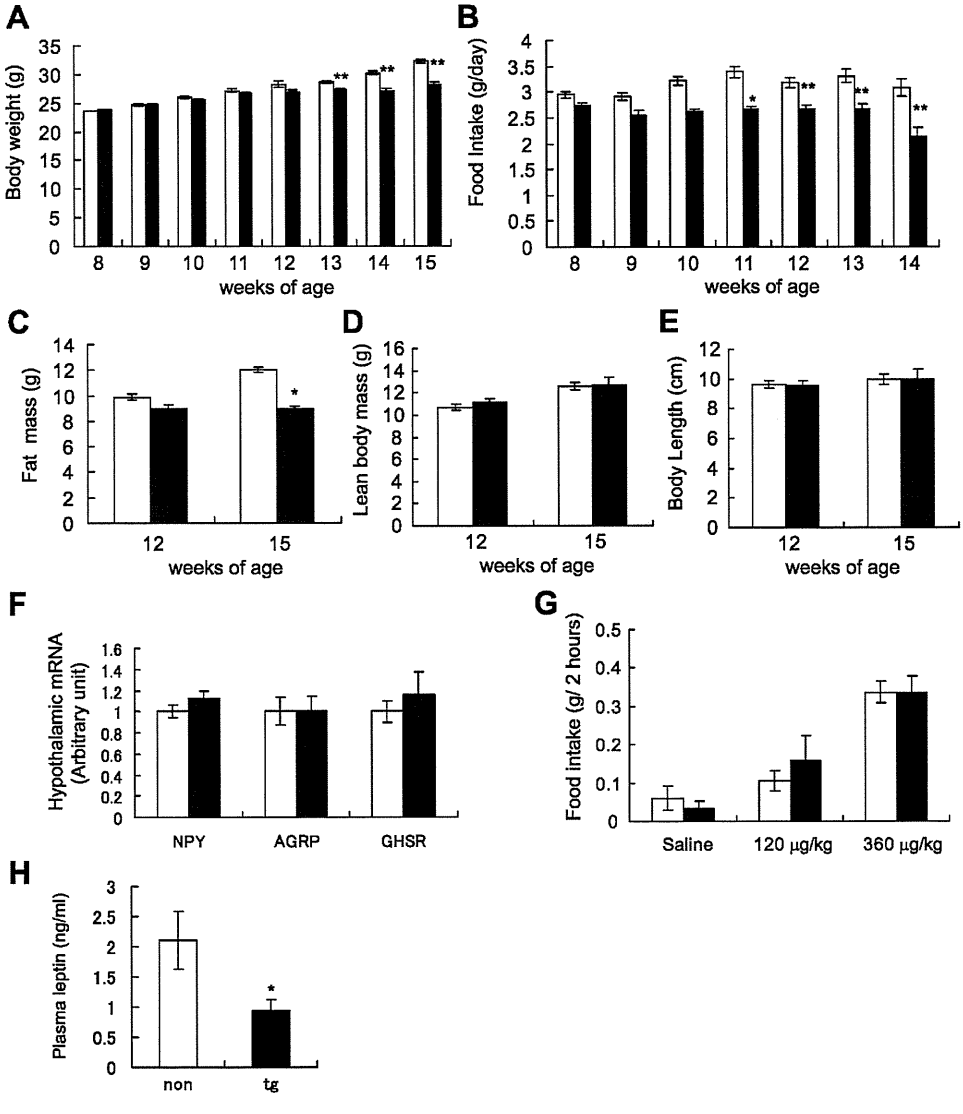

Fig. 4. Body weights, body compositions, and food intakes of GP-Tag Tg mice. *A*: body weights of male GP-Tag Tg mice (black bars) and nontransgenic littermates (open bars); $n = 22–34$. *B*: daily food intakes of male GP-Tag Tg mice (black bars) and nontransgenic littermates (open bars); $n = 19–26$. *C* and *D*: fat mass (*C*) and lean body mass (*D*) determined by animal computed tomography scan of 15-wk-old male GP-Tag Tg mice (black bars) and nontransgenic littermates (open bars). *E*: body length of 15-wk-old male GP-Tag Tg mice (black bars) and nontransgenic littermates (open bars); $n = 7–9$. *F*: hypothalamic mRNA levels of neuropeptide Y (NPY), agouti-related protein (AgRP), and growth hormone secretagogue receptor (GHS-R) in 12-wk-old male GP-Tag Tg mice (black bars) and nontransgenic littermates (open bars); $n = 7$. *G*: food intake for 2 h after injection of ghrelin (120 or 360 μg/kg or saline; $n = 10–18$). *H*: plasma leptin levels in 15-wk-old male Tg mice (black bars) and non littermates (open bars); $n = 6–7$. $^*P < 0.05$, $^{**}P < 0.01$ compared with nontransgenic littermates.

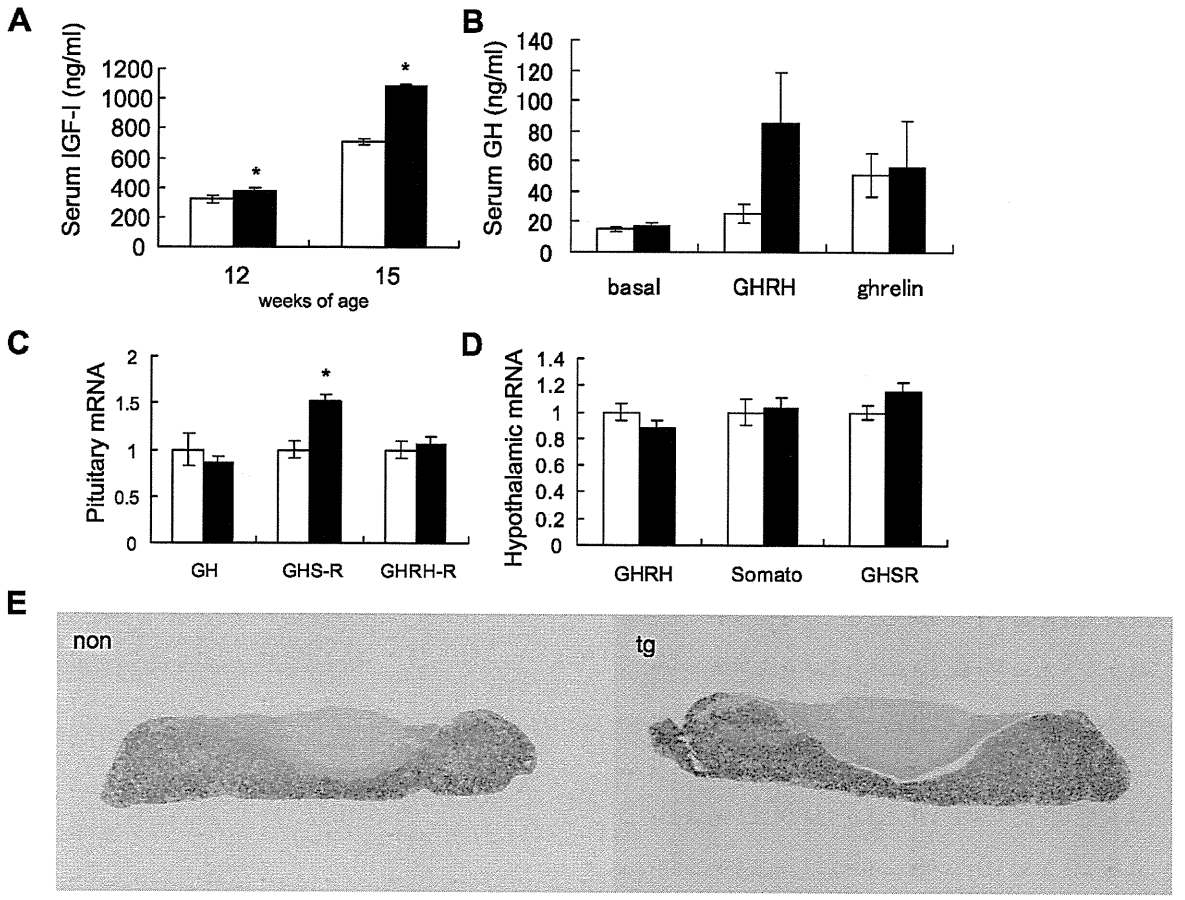

Fig. 5. GH-IGF-I axis in GP-Tag Tg mice. *A*: serum IGF-I levels in male GP-Tag Tg mice (black bars) and nontransgenic littermates (open bars); $n = 7–8$. *B*: serum GH levels at basal state and at 15 min after subcutaneous injection of GH-releasing hormone (GHRH) or ghrelin in male GP-Tag Tg mice (black bars) and nontransgenic littermates (open bars); $n = 8–13$. *C*: pituitary mRNA levels of GH, GHS-R, and GHRH-R in 15-wk-old male GP-Tag Tg mice (black bars) and nontransgenic littermates (open bars); $n = 7$. *D*: hypothalamic mRNA levels of GHRH, somatostatin (somato), and GHS-R in 15-wk-old male GP-Tag Tg mice (black bars) and nontransgenic littermates (open bars); $n = 7$. *E*: pituitary sections of 15-wk-old male Tg mice and non littermates immunostained with anti-GH antibody. *$P < 0.05$ compared with non littermates.

(NS, $n = 7$; Fig. 5, *C* and *D*). Although plasma ghrelin level was elevated, pituitary GHS-R mRNA level was upregulated in GP-Tag Tg mice ($P < 0.05$, $n = 7$; Fig. 5*C*). We also examined pituitaries of 15-wk-old male GP-Tag Tg mice by immunohistochemical analysis. There were no obvious differences in somatotroph cell number or staining intensity of GH between GP-Tag Tg mice and nontransgenic littermates (Fig. 5*E*).

Glucose metabolism in GP-Tag Tg mice. Blood glucose levels of 15-wk-old male GP-Tag Tg mice were significantly higher than controls ($P < 0.05$, $n = 10$; Fig. 6*A*), although those of 9-wk-old male GP-Tag Tg mice were comparable with the controls (non-Tg vs. Tg: 96.0 ± 4.7 vs. 100.6 ± 4.7, $P = 0.51$, $n = 9$). Intraperitoneal glucose tolerance tests showed significantly higher blood glucose levels in 15-wk-old male GP-Tag Tg mice ($P < 0.05$, $n = 6–11$; Fig. 6*B*). To estimate the insulin sensitivity of GP-Tag Tg mice, we performed an insulin tolerance test. The blood glucose levels after insulin injection in 15-wk-old male GP-Tag Tg mice were suppressed to the same level of those in controls (NS, $n = 5–8$; Fig. 6*C*). Although basal insulin levels of 15-wk-old male GP-Tag Tg mice were not significantly different from those of control mice, those after glucose injection were significantly suppressed in GP-Tag Tg mice ($P < 0.05$, $n = 7–8$; Fig. 6*D*). Pancreatic mRNA and protein levels of insulin in GP-Tag Tg were comparable with those of nontransgenic littermates (NS, $n = 6–8$; Fig. 6, *E* and *F*).

DISCUSSION

In this study, we successfully established a mouse model of ghrelinoma, GP-Tag Tg mouse. GP-Tag Tg mice exhibited chronic elevation of circulating ghrelin with physiological regulation. The elevation of circulating ghrelin in GP-Tag Tg mice (~10-fold elevation) was much higher than that in bacterial artificial chromosome transgenic mice created by Bewick et al. (5) (only ~1.5-fold elevation). Nevertheless, the levels of circulating ghrelin in GP-Tag Tg mice can be considered to be within the physiological range since the highest level of plasma ghrelin observed in the anorexia patients is about seven times higher than those of normal controls (3). One may be confused by low ghrelin mRNA levels and low ghrelin production per milligram of tissue in the stomachs of GP-Tag Tg mice. In general, when the cell cycle progresses, endocrine cell produces far less amounts of hormone since the hormone production occurs mainly at the G_0/G_1 phase of the cell cycle. Since the hyperproliferaing ghrelin-producing cells in GP-Tag Tg mice were forced to proliferate by SV40 T-antigen, which suppresses RB protein and p53, promoting cell cycle progres-

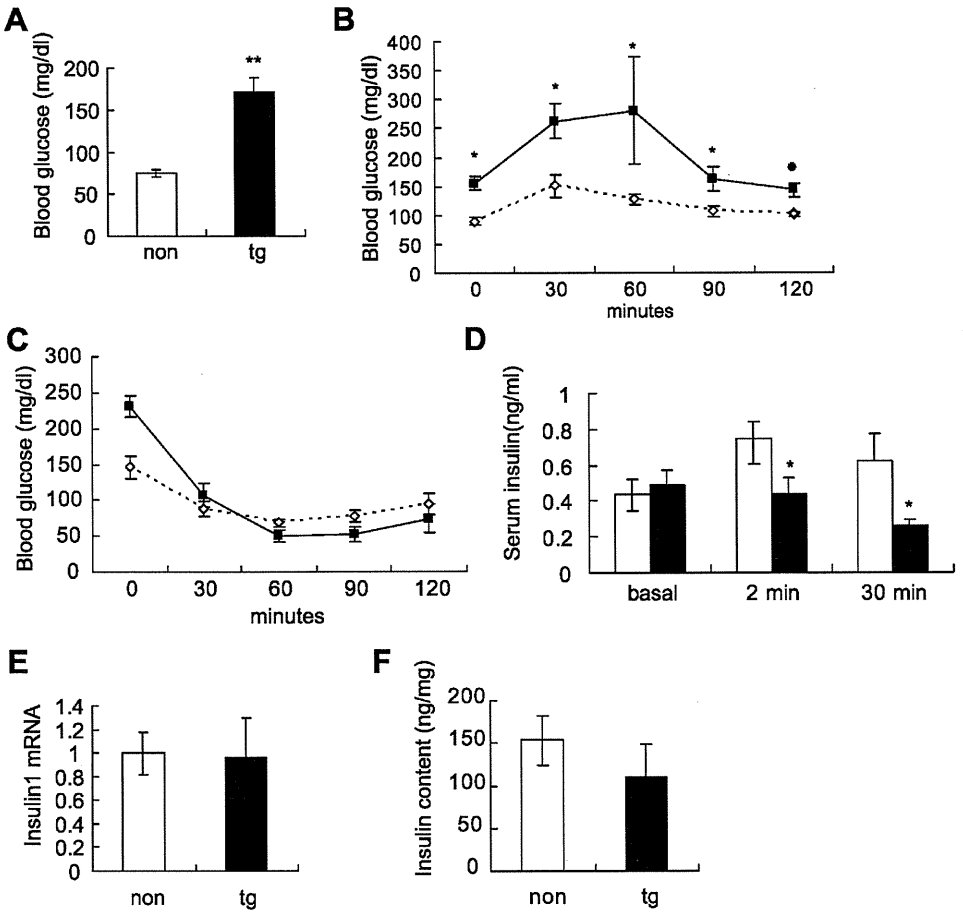

Fig. 6. Glucose metabolism in GP-Tag Tg mice. *A*: fasting blood glucose levels in 15-wk-old male Tg (black bar) and in non (open bar); n = 7–10. *B*: glucose tolerance tests in 15-wk-old male GP-Tag Tg mice (■) and in their nontransgenic littermates (◇); n = 6–11. *C*: insulin tolerance tests in male GP-Tag Tg mice (■) and in their nontransgenic littermates (◇); n = 5–8. *D*: serum insulin levels at basal, at 2 min, and at 30 min after intraperitoneal glucose injection in 15-wk-old male GP-Tag Tg mice (black bars) and in their nontransgenic littermates (open bars); n = 7–8. *E* and *F*: the mRNA (*E*) and the protein levels (*F*) of insulin in the pancreata of 15-wk-old male Tg mice (black bars) and in their non littermates (open bars); n = 6–8. *$P < 0.05$, **$P < 0.01$ compared with nontransgenic littermates.

sion, the amount of ghrelin production per cell was low. However, since the cell number was extremely increased, the net product by stomach was eventually elevated.

Several lines of evidence suggest that the GH-IGF-I axis is suppressed in the decreased GHS-R signaling state (28, 32). It has not yet been clear, however, whether chronic elevation of ghrelin within the physiological range could stimulate the GH-IGF-I axis. In this study, we found that adult GP-Tag Tg mice with elevated circulating ghrelin level showed elevated serum IGF-I level. Serum IGF-I level is regulated not only by GH but also by nutritional status. Malnutrition suppresses serum IGF-I level, whereas overnutrition elevates it (16). Since the nutritional state of GP-Tag Tg mice was poor because of decreased food intake, the elevated serum IGF-I levels in adult GP-Tag Tg mice are considered not to be due to overnutrition but to be due to activation of GH-IGF-I axis. Our findings indicate that chronic elevation of circulating ghrelin within the physiological range can activate the GH-IGF-I axis. As far as we know, this is the first report demonstrating that increased levels of circulating ghrelin within the physiological range can elevate serum IGF-I levels in rodent.

The GH-releasing action of ghrelin requires GHRH (11), and when coadministered, synergistic effects can be observed (13). Since GH responses to GHRH tended to be enhanced in adult GP-Tag Tg, the activation of the GH-IGF-I axis in GP-Tag Tg may be in part due to potentiation of the GH-releasing effect of GHRH. When the mRNA levels of components of GH regulation in pituitary and hypothalamus of GP-Tag Tg mice were investigated, an elevation of the pituitary GHS-R mRNA level was found. It is not clear whether this elevation of GHS-R mRNA in the pituitary contributes to the activated GH-IGF-I axis, since the GH response to ghrelin was not changed in GP-Tag Tg mice. At least these findings indicate that desensitization of GH secretion to ghrelin or downregulation of GHS-R did not occur by chronic elevation of circulating ghrelin in GP-Tag Tg mice.

Adult GP-Tag Tg mice exhibited high glucose level in the basal state and by the glucose tolerance test. Although insulin production was not decreased in the pancreata of GP-Tag Tg mice, insulin secretion after glucose load was significantly attenuated. Since the insulin sensitivity of GP-Tag Tg mice was not reduced, the glucose intorelance in GP-Tag Tg mice was due mainly to the decreased insulin secretion. Given that GP-Tag Tg mice have gastric tumors, there is a possibility that the glucose intorelance is due to the tumors. However, the glucose intolerance observed in malignancy is due mainly to insulin resistance (8, 15), which may be evoked by cytokines (22, 24, 27). Since the glucose intolerance of GP-Tag Tg mice was caused mainly by decreased insulin secretion, it seems not to be the case. It has been reported that acute injection of ghrelin induces suppression of insulin secretion in rodents and humans (6, 30). Our findings suggest that chronic elevation of circulating ghrelin within the physiological range leads to glucose intorelance by suppressing insulin secretion.

There have been several reports regarding ghrelin-producing tumors (9, 17, 36, 37). Most of the cases did not present

elevated plasma ghrelin levels except for a few cases. A malignant ghrelinoma case reported by Tsolakis et al. (36) showed elevated plasma ghrelin level. This patient maintained his weight despite progression of the tumor, a symptom that might be linked to the elevated ghrelin level. During the clinical course, he developed severe diabetes mellitus, which is consistent with the phenotype of GP-Tag Tg mice. GH and IGF-I levels were normal in this case. A pancreatic ghrelinoma case reported by Corbetta et al. (9) also showed normal GH and IGF-I levels despite elevated plasma ghrelin level. In contrast to these human ghrelinoma cases, GP-Tag Tg mice showed elevated IGF-I levels. The cause of the difference in the GH-IGF-I levels between our mice and these human ghrelinoma cases is unclear. Since the first case mentioned above was a malignant gastric ghrelinoma with liver metastasis, and the second case was of pancreatic origin, plasma ghrelin level might be elevated without any physiological regulation in these cases, although detailed plasma ghrelin level changes were not documented. Considering that the physiological regulation of ghrelin secretion was kept in GP-Tag Tg mice, the circadian rhythm may be needed for ghrelin to keep stimulating the GH-IGF-I axis. Indeed, several reports have shown that chronic treatment of ghrelin attenuates GH response both in vivo and in vitro (35, 39) and that in vitro treatment of pituitary with ghrelin results in decreased GHS-R mRNA levels (21). Further case studies will be required to reveal the relationship between plasma ghrelin levels and the GH-IGF-I axis in human ghrelinoma patients.

The limitation of this study is that the assessment of orexigenic action of ghrelin is difficult in this mouse model since stomach walls of GP-Tag Tg mice gradually become hypertrophic after 9 wk of age, which might affect the feeding behavior. Indeed, GP-Tag Tg mice exhibited decreased food intake and weight reduction despite the elevated plasma ghrelin levels. The hypothalamic mRNA levels of NPY and AgRP, which mediate the orexigenic action of ghrelin (7, 31), were not upregulated in GP-Tag Tg mice. There is a possibility that desensitization of GHS-R to chronic elevated ghrelin may be a cause of the lack of activation of these neurons besides the hypertrophy of the stomach wall. However, hypothalamic mRNA level of GHS-R was not changed. Furthermore, the food intake induced by acute ghrelin administration in GP-Tag Tg mice was comparable with control. These results may not support the idea of desensitization. Leptin and ghrelin have opposing effects on food intake. We examined whether plasma leptin levels of GP-Tag Tg mice were elevated as a compensation for the chronically elevated plasma ghrelin levels, which may cause anorexia. However, the leptin levels were decreased, provably reflecting the decreased fat mass of GP-Tag Tg mice.

In summary, we developed a mouse model of ghrelinoma, GP-Tag Tg mice, in which ghrelin concentrations were significantly elevated in adulthood. These GP-Tag Tg mice exhibited elevated IGF-I levels despite poor nutrition and glucose intolerance due to decreased insulin secretion. These characteristic features of this ghrelinoma mouse could be a guide to diagnose ghrelinoma.

ACKNOWLEDGMENTS

We thank Chieko Ishimoto and Chinami Shiraiwa for excellent technical assistance.

GRANTS

This study was supported by funds from the Ministry of Education, Culture, Sports, Science, and Technology of Japan and the Ministry of Health, Labour, and Welfare of Japan, a research grant from the Program for Promotion of Fundamental Studies in Health Sciences of the National Institute of Biomedical Innovation, and the Takeda Scientific Foundation in Japan.

REFERENCES

1. **Akamizu T, Shinomiya T, Irako T, Fukunaga M, Nakai Y, Kangawa K.** Separate measurement of plasma levels of acylated and desacyl ghrelin in healthy subjects using a new direct ELISA assay. *J Clin Endocrinol Metab* 90: 6–9, 2005.
2. **Ariyasu H, Takaya K, Iwakura H, Hosoda H, Akamizu T, Arai Y, Kangawa K, Nakao K.** Transgenic mice overexpressing des-acyl ghrelin show small phenotype. *Endocrinology* 146: 355–364, 2005.
3. **Ariyasu H, Takaya K, Tagami T, Ogawa Y, Hosoda K, Akamizu T, Suda M, Koh T, Natsui K, Toyooka S, Shirakami G, Usui T, Shimatsu A, Doi K, Hosoda H, Kojima M, Kangawa K, Nakao K.** Stomach is a major source of circulating ghrelin, and feeding state determines plasma ghrelin-like immunoreactivity levels in humans. *J Clin Endocrinol Metab* 86: 4753–4758, 2001.
4. **Asakawa A, Inui A, Fujimiya M, Sakamaki R, Shinfuku N, Ueta Y, Meguid MM, Kasuga M.** Stomach regulates energy balance via acylated ghrelin and desacyl ghrelin. *Gut* 54: 18–24, 2005.
5. **Bewick GA, Kent A, Campbell D, Patterson M, Ghatei MA, Bloom SR, Gardiner JV.** Mice with hyperghrelinemia are hyperphagic and glucose intolerant and have reduced leptin sensitivity. *Diabetes* 58: 840–846, 2009.
6. **Broglio F, Arvat E, Benso A, Gottero C, Muccioli G, Papotti M, van der Lely AJ, Deghenghi R, Ghigo E.** Ghrelin, a natural GH secretagogue produced by the stomach, induces hyperglycemia and reduces insulin secretion in humans. *J Clin Endocrinol Metab* 86: 5083–5086, 2001.
7. **Chen HY, Trumbauer ME, Chen AS, Weingarth DT, Adams JR, Frazier EG, Shen Z, Marsh DJ, Feighner SD, Guan XM, Ye Z, Nargund RP, Smith RG, Van der Ploeg LH, Howard AD, MacNeil DJ, Qian S.** Orexigenic action of peripheral ghrelin is mediated by neuropeptide Y and agouti-related protein. *Endocrinology* 145: 2607–2612, 2004.
8. **Copeland GP, Leinster SJ, Davis JC, Hipkin LJ.** Insulin resistance in patients with colorectal cancer. *Br J Surg* 74: 1031–1035, 1987.
9. **Corbetta S, Peracchi M, Cappiello V, Lania A, Lauri E, Vago L, Beck-Peccoz P, Spada A.** Circulating ghrelin levels in patients with pancreatic and gastrointestinal neuroendocrine tumors: identification of one pancreatic ghrelinoma. *J Clin Endocrinol Metab* 88: 3117–3120, 2003.
10. **Date Y, Kojima M, Hosoda H, Sawaguchi A, Mondal MS, Suganuma T, Matsukura S, Kangawa K, Nakazato M.** Ghrelin, a novel growth hormone-releasing acylated peptide, is synthesized in a distinct endocrine cell type in the gastrointestinal tracts of rats and humans. *Endocrinology* 141: 4255–4261, 2000.
11. **Dimaraki EV, Jaffe CA.** Role of endogenous ghrelin in growth hormone secretion, appetite regulation and metabolism. *Rev Endocr Metab Disord* 7: 237–249, 2006.
12. **Gutierrez JA, Solenberg PJ, Perkins DR, Willency JA, Knierman MD, Jin Z, Witcher DR, Luo S, Onyia JE, Hale JE.** Ghrelin octanoylation mediated by an orphan lipid transferase. *Proc Natl Acad Sci USA* 105: 6320–6325, 2008.
13. **Hataya Y, Akamizu T, Takaya K, Kanamoto N, Ariyasu H, Saijo M, Moriyama K, Shimatsu A, Kojima M, Kangawa K, Nakao K.** A low dose of ghrelin stimulates growth hormone (GH) release synergistically with GH-releasing hormone in humans. *J Clin Endocrinol Metab* 86: 4552, 2001.
14. **Hosoda H, Kojima M, Matsuo H, Kangawa K.** Ghrelin and des-acyl ghrelin: two major forms of rat ghrelin peptide in gastrointestinal tissue. *Biochem Biophys Res Commun* 279: 909–913, 2000.
15. **Isaksson B, Strommer L, Friess H, Buchler MW, Herrington MK, Wang F, Zierath JR, Wallberg-Henriksson H, Larsson J, Permert J.** Impaired insulin action on phosphatidylinositol 3-kinase activity and glucose transport in skeletal muscle of pancreatic cancer patients. *Pancreas* 26: 173–177, 2003.
16. **Iwakura H, Akamizu T, Ariyasu H, Irako T, Hosoda K, Nakao K, Kangawa K.** Effects of ghrelin administration on decreased growth hormone status in obese animals. *Am J Physiol Endocrinol Metab* 293: E819–E825, 2007.

17. **Iwakura H, Hosoda K, Doi R, Komoto I, Nishimura H, Son C, Fujikura J, Tomita T, Takaya K, Ogawa Y, Hayashi T, Inoue G, Akamizu T, Hosoda H, Kojima M, Kangawa K, Imamura M, Nakao K.** Ghrelin expression in islet cell tumors: augmented expression of ghrelin in a case of glucagonoma with multiple endocrine neoplasm type I. *J Clin Endocrinol Metab* 87: 4885–4888, 2002.
18. **Iwakura H, Hosoda K, Son C, Fujikura J, Tomita T, Noguchi M, Ariyasu H, Takaya K, Masuzaki H, Ogawa Y, Hayashi T, Inoue G, Akamizu T, Hosoda H, Kojima M, Itoh H, Toyokuni S, Kangawa K, Nakao K.** Analysis of rat insulin II promoter-ghrelin transgenic mice and rat glucagon promoter-ghrelin transgenic mice. *J Biol Chem* 280: 15247–15256, 2005.
19. **Kanamoto N, Akamizu T, Tagami T, Hataya Y, Moriyama K, Takaya K, Hosoda H, Kojima M, Kangawa K, Nakao K.** Genomic structure and characterization of the 5′-flanking region of the human ghrelin gene. *Endocrinology* 145: 4144–4153, 2004.
20. **Kojima M, Hosoda H, Date Y, Nakazato M, Matsuo H, Kangawa K.** Ghrelin is a growth-hormone-releasing acylated peptide from stomach. *Nature* 402: 656–660, 1999.
21. **Luque RM, Kineman RD, Park S, Peng XD, Gracia-Navarro F, Castano JP, Malagon MM.** Homologous and heterologous regulation of pituitary receptors for ghrelin and growth hormone-releasing hormone. *Endocrinology* 145: 3182–3189, 2004.
22. **Makino T, Noguchi Y, Yoshikawa T, Doi C, Nomura K.** Circulating interleukin 6 concentrations and insulin resistance in patients with cancer. *Br J Surg* 85: 1658–1662, 1998.
23. **Masuda Y, Tanaka T, Inomata N, Ohnuma N, Tanaka S, Itoh Z, Hosoda H, Kojima M, Kangawa K.** Ghrelin stimulates gastric acid secretion and motility in rats. *Biochem Biophys Res Commun* 276: 905–908, 2000.
24. **McCall JL, Tuckey JA, Parry BR.** Serum tumour necrosis factor alpha and insulin resistance in gastrointestinal cancer. *Br J Surg* 79: 1361–1363, 1992.
25. **Nagaya N, Kojima M, Uematsu M, Yamagishi M, Hosoda H, Oya H, Hayashi Y, Kangawa K.** Hemodynamic and hormonal effects of human ghrelin in healthy volunteers. *Am J Physiol Regul Integr Comp Physiol* 280: R1483–R1487, 2001.
26. **Nakazato M, Murakami N, Date Y, Kojima M, Matsuo H, Kangawa K, Matsukura S.** A role for ghrelin in the central regulation of feeding. *Nature* 409: 194–198, 2001.
27. **Noguchi Y, Yoshikawa T, Marat D, Doi C, Makino T, Fukuzawa K, Tsuburaya A, Satoh S, Ito T, Mitsuse S.** Insulin resistance in cancer patients is associated with enhanced tumor necrosis factor-alpha expression in skeletal muscle. *Biochem Biophys Res Commun* 253: 887–892, 1998.
28. **Pantel J, Legendre M, Cabrol S, Hilal L, Hajaji Y, Morisset S, Nivot S, Vie-Luton MP, Grouselle D, de Kerdanet M, Kadiri A, Epelbaum J, Le Bouc Y, Amselem S.** Loss of constitutive activity of the growth hormone secretagogue receptor in familial short stature. *J Clin Invest* 116: 760–768, 2006.
29. **Reed JA, Benoit SC, Pfluger PT, Tschöp MH, D'Alessio DA, Seeley RJ.** Mice with chronically increased circulating ghrelin develop age-related glucose intolerance. *Am J Physiol Endocrinol Metab* 294: E752–E760, 2008.
30. **Reimer MK, Pacini G, Ahren B.** Dose-dependent inhibition by ghrelin of insulin secretion in the mouse. *Endocrinology* 144: 916–921, 2003.
31. **Shintani M, Ogawa Y, Ebihara K, Aizawa-Abe M, Miyanaga F, Takaya K, Hayashi T, Inoue G, Hosoda K, Kojima M, Kangawa K, Nakao K.** Ghrelin, an endogenous growth hormone secretagogue, is a novel orexigenic peptide that antagonizes leptin action through the activation of hypothalamic neuropeptide Y/Y1 receptor pathway. *Diabetes* 50: 227–232, 2001.
32. **Shuto Y, Shibasaki T, Otagiri A, Kuriyama H, Ohata H, Tamura H, Kamegai J, Sugihara H, Oikawa S, Wakabayashi I.** Hypothalamic growth hormone secretagogue receptor regulates growth hormone secretion, feeding, and adiposity. *J Clin Invest* 109: 1429–1436, 2002.
33. **Tack J, Depoortere I, Bisschops R, Delporte C, Coulie B, Meulemans A, Janssens J, Peeters T.** Influence of ghrelin on interdigestive gastrointestinal motility in humans. *Gut* 55: 327–333, 2006.
34. **Takaya K, Ariyasu H, Kanamoto N, Iwakura H, Yoshimoto A, Harada M, Mori K, Komatsu Y, Usui T, Shimatsu A, Ogawa Y, Hosoda K, Akamizu T, Kojima M, Kangawa K, Nakao K.** Ghrelin strongly stimulates growth hormone release in humans. *J Clin Endocrinol Metab* 85: 4908–4911, 2000.
35. **Thompson NM, Davies JS, Mode A, Houston PA, Wells T.** Pattern-dependent suppression of growth hormone (GH) pulsatility by ghrelin and GH-releasing peptide-6 in moderately GH-deficient rats. *Endocrinology* 144: 4859–4867, 2003.
36. **Tsolakis AV, Portela-Gomes GM, Stridsberg M, Grimelius L, Sundin A, Eriksson BK, Oberg KE, Janson ET.** Malignant gastric ghrelinoma with hyperghrelinemia. *J Clin Endocrinol Metab* 89: 3739–3744, 2004.
37. **Volante M, Allia E, Gugliotta P, Funaro A, Broglio F, Deghenghi R, Muccioli G, Ghigo E, Papotti M.** Expression of ghrelin and of the GH secretagogue receptor by pancreatic islet cells and related endocrine tumors. *J Clin Endocrinol Metab* 87: 1300–1308, 2002.
38. **Wei W, Qi X, Reed J, Ceci J, Wang HQ, Wang G, Englander EW, Greeley GH Jr.** Effect of chronic hyperghrelinemia on ingestive action of ghrelin. *Am J Physiol Regul Integr Comp Physiol* 290: R803–R808, 2006.
39. **Yamazaki M, Nakamura K, Kobayashi H, Matsubara M, Hayashi Y, Kangawa K, Sakai T.** Regulational effect of ghrelin on growth hormone secretion from perifused rat anterior pituitary cells. *J Neuroendocrinol* 14: 156–162, 2002.
40. **Yang J, Brown MS, Liang G, Grishin NV, Goldstein JL.** Identification of the acyltransferase that octanoylates ghrelin, an appetite-stimulating peptide hormone. *Cell* 132: 387–396, 2008.
41. **Zhang W, Chai B, Li JY, Wang H, Mulholland MW.** Effect of des-acyl ghrelin on adiposity and glucose metabolism. *Endocrinology* 149: 4710–4716, 2008.

Guanylyl Cyclase-A Inhibits Angiotensin II Type 2 Receptor-Mediated Pro-Hypertrophic Signaling in the Heart

Yuhao Li, Yoshihiko Saito, Koichiro Kuwahara, Xianglu Rong, Ichiro Kishimoto, Masaki Harada, Yuichiro Adachi, Michio Nakanishi, Hideyuki Kinoshita, Masatsugu Horiuchi, Michael Murray, and Kazuwa Nakao

Department of Medicine and Clinical Science (Y.L., K.K., X.R., M.H., Y.A., M.N., H.K., K.N.), Kyoto University Graduate School of Medicine, Kyoto 606-8507, Japan; First Department of Internal Medicine (Y.S.), Nara Medical University, Nara 634, Japan; National Cardiovascular Center Research Institute (I.K.), Osaka 565-8565, Japan; Department of Molecular Cardiovascular Biology and Pharmacology (M.H.), Ehime University Graduate School of Medicine, Ehime 791-0295, Japan; and Faculty of Pharmacy (M.M.), The University of Sydney, Sydney, New South Wales 2006, Australia

Angiotensin II plays a key role in the development of cardiac hypertrophy. The contribution of the angiotensin II type 1 receptor (AT1) in angiotensin II-induced cardiac hypertrophy is well established, but the role of AT2 signaling remains controversial. Previously, we have shown that natriuretic peptide receptor/guanylyl cyclase-A (GCA) signaling protects the heart from hypertrophy at least in part by inhibiting AT1-mediated pro-hypertrophic signaling. Here, we investigated the role of AT2 in cardiac hypertrophy observed in mice lacking GCA. Real-time RT-PCR and immunoblotting approaches indicated that the cardiac AT2 gene was overexpressed in GCA-deficient mice. Mice lacking AT2 alone did not exhibit an abnormal cardiac phenotype. In contrast, GCA-deficiency-induced increases in heart to body weight ratio, cardiomyocyte cross-sectional area, and collagen accumulation as evidenced by van Gieson staining were attenuated when AT2 was absent. Furthermore, the up-regulated cardiac expression of hypertrophy-related genes in GCA-null animals was also suppressed. Pharmacological blockade of AT2 with PD123319 similarly attenuated cardiac hypertrophy in GCA-deficient mice. In addition, whereas the AT1 antagonist olmesartan attenuated cardiac hypertrophy in GCA-deficient mice, this treatment was without effect on cardiac hypertrophy in GCA/AT2-double null mice, notwithstanding its potent antihypertensive effect in these animals. These results suggest that the interplay of AT2 and AT1 may be important in the development of cardiac hypertrophy. Collectively, our findings support the assertion that GCA inhibits AT2-mediated pro-hypertrophic signaling in heart and offer new insights into endogenous cardioprotective mechanisms during disease pathogenesis. (***Endocrinology*** **150: 3759–3765, 2009)**

Cardiac hypertrophy is an independent risk factor for cardiac morbidity and mortality. Left ventricular hypertrophy is a major, independent predictor of cardiovascular events, particularly in hypertension, in which it dramatically increases the risk of stroke, coronary heart disease, and heart failure (1). Therefore, elucidation of the underlying mechanism leading to cardiac hypertrophy may have significant implications for the development of therapeutic strategies.

Atrial natriuretic peptide (ANP) is a cardiac hormone that acts through guanylate cyclase-A (GCA) to lower blood pressure and dilate blood vessels *in vivo* (2) and to inhibit the growth of cardiac myocytes and fibroblasts *in vitro* (3). Brain natriuretic peptide (BNP) also activates GCA and has effects similar to those of ANP, although it also exerts local antifibrotic actions in the ventricle (4). Mice lacking GCA exhibit hypertension, cardiac hypertrophy, and fibrosis and are prone to sudden death, which is consistent with a protective role for natriuretic peptide/GCA-signaling pathways in the cardiovascular system (5–8).

Angiotensin (Ang) II plays a key role in the development of cardiac hypertrophy (9). Although most of the cardiovascular

ISSN Print 0013-7227 ISSN Online 1945-7170
Printed in U.S.A.

doi: 10.1210/en.2008-1353 Received September 18, 2008. Accepted April 6, 2009.
First Published Online April 16, 2009

Abbreviations: ACE, Angiotensin converting enzyme; Agt, angiotensinogen; Ang, angiotensin; ANP, atrial natriuretic peptide; AT1, angiotensin II type 1 receptor; BNP, brain natriuretic peptide; BW, body weight; GCA, guanylyl cyclase-A; HW, heart weight; KO, knockout; LVW, left ventricular weight; NPR, natriuretic peptide receptor; RVW, right ventricular weight; SBP, systolic blood pressure; WT, wild type.

effects of Ang II are mediated via the Ang II type 1 receptor (AT1) (10), the alternate major Ang II receptor subtype, AT2, may also be important because its expression is up-regulated in cardiovascular pathologies, including cardiac hypertrophy (11, 12) and heart failure (13). Although the roles of AT2 in cardiac remodeling remain controversial, accumulating lines of evidence appear to support the view that AT2 can promote cardiac growth in pathological situations. Indeed, at least in some tissues, AT1 and AT2 share common signaling pathways that stimulate cell and tissue proliferation (14–18).

We have demonstrated previously that genetic or pharmacological blockade of AT1a signaling attenuates cardiac hypertrophy and fibrosis in GCA-deficient mice (6, 7), suggesting that GCA inhibits AT1a-mediated pathological signaling in the heart. Importantly, however, the cardiac hypertrophy and fibrosis in GCA-deficient mice was not completely abolished in animals lacking both GCA and AT1a (6). Similarly, AT1 blockade by olmesartan (CS-866) in GCA-null mice only partially reversed the increase in cardiac hypertrophy and fibrosis, suggesting the involvement of AT1-independent signaling in cardiac remodeling observed in GCA-deficient mice. In the present study, we investigated the role played by AT2 in cardiac hypertrophy induced by GCA deficiency using further genetic and pharmacological manipulation in mice. The findings of this study are consistent with a pro-hypertrophic effect of AT2 signaling in heart.

Materials and Methods

Animals and treatments

All experimental procedures were performed according to Kyoto University standards for animal care.

Experiment 1

Male homozygous GCA-deficient [$GCA^{-/-}/AT2^{+/y}$, GCA knockout (KO)] and wild-type (WT, $GCA^{+/+}/AT2^{+/y}$) mice used in this experiment (n = 7 each group) were generated by methods described previously (5). The genetic backgrounds of the mice were C57BL/6. Animals at 16–17 wk of age were killed for initial gene analysis.

Experiment 2

The genetic backgrounds of the AT2-deficient ($GCA^{+/+}/AT2^{-/y}$, AT2 KO) mice were FVB/N. Male homozygous AT2 KO, GCA KO, $GCA^{-/-}/AT2^{-/y}$ (double KO), and WT mice used in this experiment (n = 7–9 each group) were generated from the heterozygotes after crossing female AT2 KO and male GCA KO mice. Systolic blood pressure (SBP) was measured at 11, 14, and 16 wk of age using a noninvasive computerized tail-cuff method (BP98A; Softron Co., Ltd., Tokyo, Japan) (6–8). Animals at 16–17 wk of age were killed for further examination.

Experiment 3

WT and GCA KO mice were used in this experiment (n = 5 each group). The AT2 antagonist PD123319 (30 mg/kg · d; Sigma, Osaka, Japan) was dissolved in saline and administered daily by ip injection for 4 wk, in mice at 12–13 wk of age. The corresponding control animals were treated with saline only. SBP was measured before and 2 and 3 wk after treatment with the antagonist or saline using a tail-cuff method (MK-2000ST; Muromachi Kikai Co. Ltd., Tokyo, Japan). Animals were killed for further examination after 4 wk treatment.

Experiment 4

All four genotypes were used in this experiment (n = 7–9 each group). The AT1 antagonist olmesartan (a gift from Daiichi-Sankyo Co. Ltd., Tokyo, Japan) was suspended in 5% gum arabic and administered by oral gavage at a dose of 10 mg/kg once a day for 4 wk in mice at 12–13 wk of age; control animals received vehicle alone. SBP was measured 3 wk after treatment with the antagonist or vehicle using a tail-cuff method (BP98A; Softron). Animals were killed for further examination after 4 wk treatment.

Determination of heart weight (HW) and right and left ventricular weights (RVW and LVW)

Animals were euthanized, hearts were removed and weighed, and then the right and left ventricles were weighed separately. The ratios of these weights to the total body weight (BW) (HW/BW, RVW/BW, and LVW/BW) were calculated as indexes of cardiac hypertrophy.

Measurement of cardiomyocyte cross-sectional area and histological assessment of cardiac fibrosis

A segment of the excised left ventricle from each animal was fixed in 10% neutral formalin over several days and then dehydrated with graded concentrations of alcohol before embedding in paraffin. Paraffin slices from each heart were stained with hematoxylin-eosin. Morphometry of each section was performed to determine the myocyte cross-sectional area as described previously (19). The cross-sectional area of cardiomyocytes in sections that had been cut transversely was measured using a KS400 Imaging System (Carl Zeiss Vision, Eching, Germany); cardiomyocytes possessed an intact cellular membrane, and the nucleus was visible. The outer borders of the cardiomyocytes were traced at × 400 magnification, and the cardiomyocyte areas were calculated. One hundred cells per heart were counted, and the mean value was used in subsequent analyses.

To determine the extent of collagen fiber accumulation, paraffin slices from each heart were subjected to van Gieson staining. Forty fields from three individual sections were selected at random, and the van Gieson-stained areas were measured in relation to the total left ventricular area using image analysis software and a Zeiss KS400 system (6, 7).

Analysis of mRNA

Total RNA was prepared from individual left ventricles of mouse hearts using TRIzol (Life Technologies Inc., Rockville, MD). mRNAs were quantified by real-time RT-PCR using the TaqMan system (ABI PRISM 7700 Sequence Detector; Applied Biosystems, Foster City, CA) (6). The primers and probes of the genes examined were as follows: ANP sense 5′-GCCATATTGGAGCAAATCCT-3′, antisense 5′-GCAGGTTCTTGAAATCCATCA-3′, and oligonucleotide probe, 5′-TGTACAGTGCGGTGTCCAACACAGAT-3′; BNP sense 5′-CCAGTCTCCAGAGCAATTCAA-3′, antisense 5′-GCCATTTCCTCCGACTTTT-3′, and oligonucleotide probe 5′-TGCAGAAGCTGCTGGAGCTGATAAGA-3′; collagen I sense 5′-GTCCCAACCCCCAAAGAC-3′, antisense 5′-CATCTTCTGAGTTTGGTGATACGT-3′, and oligonucleotide probe 5′-CACGGCTGTGTGCGATGACG-3′; collagen III sense 5′-TGGTTTCTTCTCACCCTTCTTC-3′, antisense 5′-TGCATCCCAATTCATCTACGT-3′, and oligonucleotide probe 5′-TCCCACTCTTATTTTGGCACAGCAGTC-3′; angiotensinogen (Agt) sense 5′-CATTGGTGACACCAACCCC-3′, antisense 5′-GCTGTTCCTCCTCTCCTGCT-3′, and oligonucleotide probe 5′-AGGTTCTCAATAGCATCCTCCTCGAACTC-3′; angiotensin converting enzyme (ACE) sense 5′-CGGAATGAAACCCATTTTGA-3′, antisense 5′-GCACAAAGCTCACGAAGTACC-3′, and oligonucleotide probe 5′-CACATCCCAAACGTGACACCGTACAT-3′; AT1a sense 5′-GTTTGCGCTTTTCATTACGAGT-3′, antisense 5′-TCTTGGTTAGGCCCAGTCCT-3′, and oligonucleotide probe 5′-CCGGAATTCAACGCTCCCCA-3′; AT2 sense 5′-CCACCA GCAGAAACATTACC-3′, antisense 5′-GGACTCATTGGTGCCAGTT-3′, and oligonucleotide probe 5′-CAGCCGTCCTTTTGATAATCTCAACG-3′; and TGF-β1 sense 5′-GACGTCACTGGAGTTGTACGG-3′, antisense 5′-GCTGA-

ATCGAAAGCCCTGT-3′, and oligonucleotide probe 5′-AGCGCATC-GAAGCCATCCG −3′. Glyceraldehyde-3-phosphate dehydrogenase (housekeeping gene) mRNA was also amplified with specific primers and probe (Applied Biosystems).

Immunoblotting

AT2 protein was estimated by Western blotting (20). Total proteins were resolved on 4–12% polyacrylamide gradient gels (Invitrogen, Carlsbad, CA), electrophoretically transferred to polyvinylidene difluoride membranes, blocked [in buffer containing 20 mM Tris (pH 7.5), 150 mM NaCl, 5% BSA, 0.1% Tween 20], and incubated for 18 h at 4 C with AT2 receptor-specific antibody (Santa Cruz Biotechnology, Santa Cruz, CA). Detection was performed with peroxidase-conjugated secondary antibody, using an ECL chemiluminescence kit (Amersham, Buckinghamshire, UK). Immunoblotting with a monoclonal anti-β-actin antibody (Cell Signaling, Beverly, MA) was conducted to ensure equal protein loading.

Statistical analysis

All results are expressed as means ± SEM of values obtained in individual animals. Data were analyzed by single-factor ANOVA. If a significant effect was found, the Fisher's protected least significant difference test was performed to isolate the difference between the groups. Student's *t* test was used to assess the effect of olmesartan treatment on the hypertrophic phenotype in GCA KO mice (see Fig. 6). A value of $P < 0.05$ was considered to be statistically significant.

Results

AT2 deficiency ameliorates cardiac hypertrophy in GCA-deficient mice

We first determined cardiac gene expression of AT2 and AT1a in WT and GCA KO mice using real-time RT-PCR analysis. The results demonstrated an increase in cardiac AT2 mRNA expression in GCA-deficient mice compared with WT controls (Fig. 1A). Western blot analysis confirmed the increase in AT2 expression in GCA-null mouse heart at the protein level (Fig. 1B). In contrast, cardiac AT1a mRNA expression did not differ between WT and GCA null mice (Fig. 1C). There were no differences in the cardiac expression of Agt and ACE between WT and GCA-KO (data not shown).

To evaluate the potential role of AT2 in cardiac hypertrophy induced by GCA deficiency, we generated mice lacking both GCA and AT2 by crossing AT2 KO and GCA KO mice. There was no significant difference in BW among the four genotypes (WT, 34.1 ± 1.1 g; AT2 KO, 34.3 ± 1.1 g; GCA KO, 35.4 ± 1.1 g; double KO, 34.3 ± 0.7 g). In accord with previous reports (15, 16, 21), single deletion of AT2 did not induce a change in cardiac phenotype (Figs. 2, A–D, and 3, A, B, D, and H). By contrast, deletion of GCA alone increased SBP (Fig. 2A), HW/BW (Fig. 2B), LVW/BW (Fig. 2C), RVW/BW (Fig. 2D), the cross-sectional area of cardiomyocytes (Fig. 3, A and E), and cardiac interstitial van Gieson-staining area (Fig. 3, B and I). Importantly, SBP was not different between GCA KO and double KO mice (Fig. 2A), whereas HW/BW, LVW/BW, and RVW/BW ratios, the cross-sectional area of cardiomyocytes, and left ventricular interstitial fibrosis were all lower in double KO mice compared with GCA KO animals (Figs. 2, B–D, and 3, A, B, F, and J).

We further examined the expression of hypertrophy-related genes. Cardiomyocytes are the major source of ANP and BNP (2), which are two important molecular markers of cardiomyocyte hypertrophy (22). Collagens I and III are the principal collagen genes expressed in heart. Consistent with the changes in cardiac hypertrophy and fibrosis, deletion of AT2 alone did not alter cardiac expression of mRNAs for ANP, BNP, and collagens I and III in mice (Fig. 4, A–D). However, the increased cardiac expression of each of these genes that was observed in mice that lacked GCA was suppressed when AT2 was also deleted (Fig. 4, A–D).

To investigate the underlying mechanism, we further examined cardiac expression of Agt, ACE, AT1a, and TGF-β1 mRNAs. No differences in the expression of Agt, ACE, and AT1a mRNAs were observed between genotypes (Fig. 4, E–G). Single

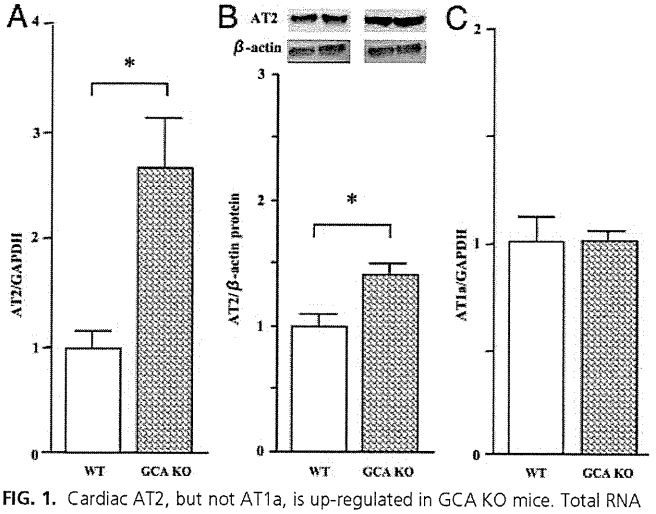

FIG. 1. Cardiac AT2, but not AT1a, is up-regulated in GCA KO mice. Total RNA was extracted from the left ventricular tissues using TRIzol. A and C, AT2 (A) and AT1a (C) mRNAs were determined by real-time RT-PCR, and the results were normalized to GAPDH. B, AT2 protein was detected by Western immunoblot analysis. Values are means ± SEM (n = 7). *, $P < 0.05$.

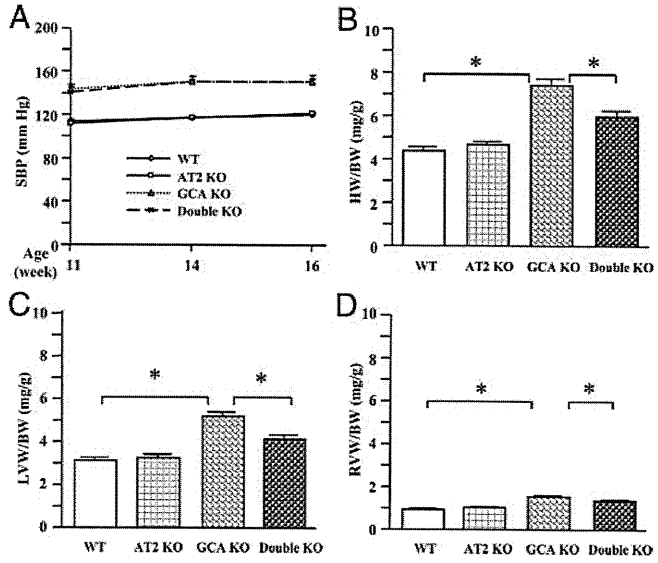

FIG. 2. Targeted deletion of AT2 ameliorated cardiac hypertrophy in GCA-deficient mice. A–D, SBP (A), HW/BW (B), LVW/BW (C), and RVW/BW (D) in WT, AT2 KO, GCA KO, and AT2/GCA double KO mice. Values are means ± SEM (n = 7–9). *, $P < 0.05$.

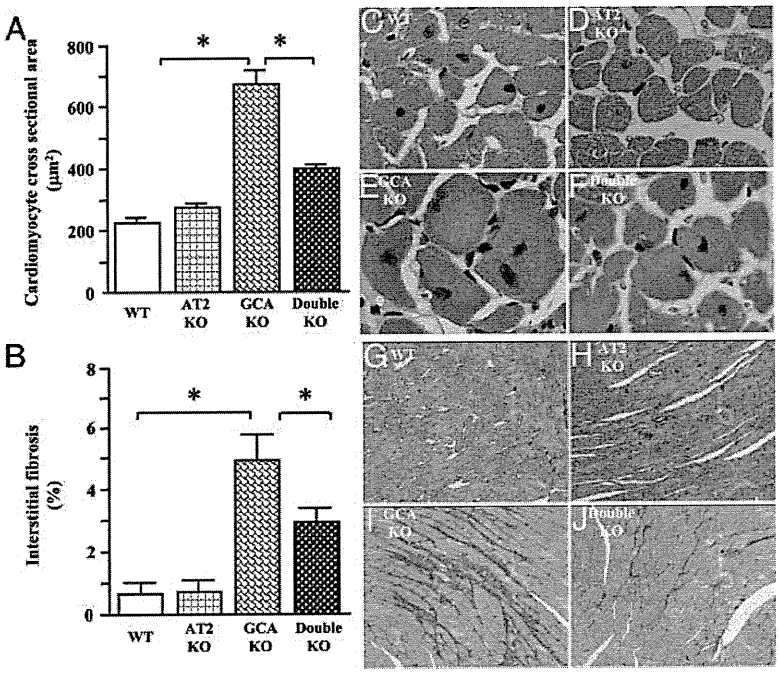

FIG. 3. Deletion of AT2 decreased cardiomyocyte cross-sectional areas and cardiac interstitial fibrosis in GCA-deficient mice. Morphometry of left ventricular myocytes was performed to measure the myocyte cross-sectional area as described previously (19). The van Gieson-stained collagen deposit area and total ventricular area in the left ventricles were analyzed using an image analyzing system. A, Cardiomyocyte cross-sectional areas in the four mouse genotypes under investigation; B, interstitial fibrosis (percent, the van Gieson-stained area to total ventricular area ratio); C–F, representative histological findings of cardiomyocytes in different experimental groups (hematoxylin-eosin staining). Magnification, ×400. G–J, Representative examples of cardiac interstitial fibrosis (*red*; ×200). Values are means ± SEM (n = 7–9). *, $P < 0.05$.

deletion of AT2 did not alter cardiac expression of TGF-β1 (Fig. 4H). However, TGF-β1 gene expression was significantly upregulated in cardiac tissues from GCA KO mice. Consistent with the observed attenuation of cardiac hypertrophy and fibrosis, TGF-β1 expression in double KO mice was returned to the levels observed in hearts from WT mice.

Pharmacological blockade of AT2 also attenuates cardiac hypertrophy in GCA-deficient mice

To substantiate the role of AT2 in GCA deficiency-induced cardiac hypertrophy, we administered the AT2 antagonist PD123319 to GCA-null mice. Consistent with genetic blockade of AT2, PD123319 treatment for 4 wk did not affect SBP (Fig. 5A) but decreased the ratios of HW/BW and LVW/BW in GCA KO mice (Fig. 5, B and C); RVW/BW ratio was unchanged (Fig. 5D).

Residual cardiac hypertrophy in double KO mice is resistant to an AT1 antagonist

Pharmacological or genetic blockade of AT1 has been shown to attenuate GCA-deficiency-induced cardiac hypertrophy (6). Although cardiac mass in double KO mice was significantly lower than in GCA KO mice, it was still greater than that in WT and AT2 KO mice (Fig. 2, B–D). To test whether the residual hypertrophic effect might be mediated by AT1, we administered the AT1 antagonist olmesartan to WT, AT2 KO, GCA KO, and double KO mice. Olmesartan treatment similarly decreased SBP in all four of the murine genotypes under investigation (Fig. 6A). However, whereas this treatment significantly reduced HW/BW (Fig. 6B) and LVW/BW (Fig. 6C) in GCA KO, it was without effect in double KO mice.

Discussion

The role of AT2-mediated signaling pathways in the development of cardiac hypertrophy remains controversial. Initially, AT2 was reported to exert opposing effects on growth-promoting signaling mediated by AT1 (23). On the other hand, there are several reports that AT2 activates pro-hypertrophic signaling in some animal models (15, 16, 18). Thus, AT2 may have complex effects in the development of cardiovascular hypertrophy (24). It has been reported that the expression of AT2, but not AT1, is directly correlated with left ventricular mass in aortic-banded rats that exhibit cardiac hypertrophy (11, 25). In accord with these reports, the present findings from real-time RT-PCR and immunoblot analyses demonstrated that AT2, but not AT1a, was upregulated in GCA KO mouse heart. Although deletion of AT2 alone did not induce a change in cardiac phenotype, the increase in cardiac mass reflected by increased ratios

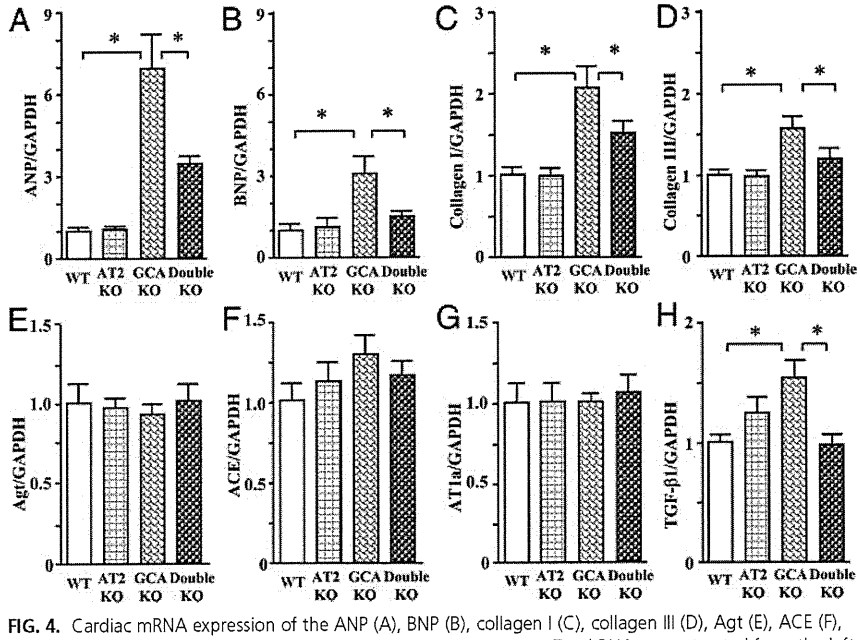

FIG. 4. Cardiac mRNA expression of the ANP (A), BNP (B), collagen I (C), collagen III (D), Agt (E), ACE (F), AT1a (G), and TGF-β1 (H) genes among different mouse genotypes. Total RNA was extracted from the left ventricular tissues using TRIzol. The relative levels of specific mRNAs were determined by real-time RT-PCR. Results were normalized to GAPDH. Values are means ± SEM (n = 7–9). *, $P < 0.05$.

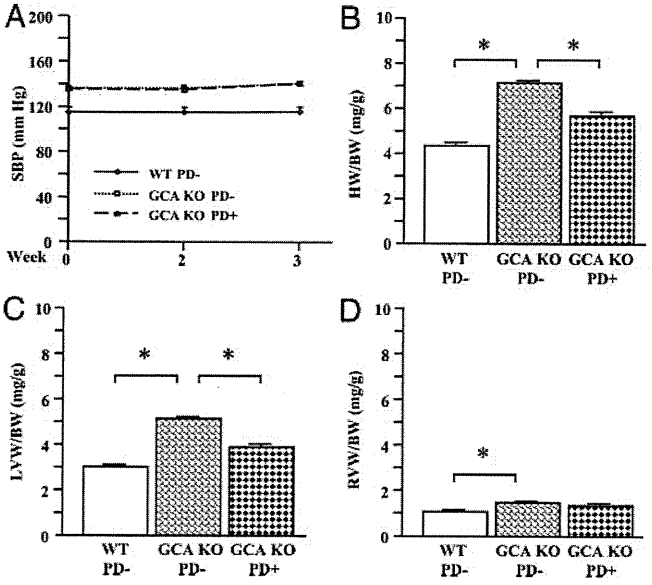

FIG. 5. Pharmacological blockade of AT2 ameliorated cardiac hypertrophy but did not affect hypertension in GCA-deficient mice. The AT2 antagonist PD123319 (30 mg/kg) was injected (ip) daily for 4 wk. The corresponding control animals were treated with saline alone. A–D, SBP (A), HW/BW (B), LVW/BW (C), and RVW/BW (D) in saline-treated (PD−) or PD123319-treated (PD+) mice. Values are means ± SEM (n = 5 each group). *, $P < 0.05$.

of cardiac weights to body weight, cardiomyocyte cross-sectional area, and collagen accumulation and overexpression of hypertrophic genes ANP, BNP, and collagens I and III in GCA-deficient hearts were all suppressed by AT2 deletion. Similarly, the cardiac hypertrophy in GCA-deficient mice was also attenuated by pharmacological blockade with PD123319. These results clearly indicate that AT2-dependent pro-hypertrophic signaling is dependent on GCA deficiency. Thus, similar to the situation with AT1a (6), AT2-mediated pro-hypertrophic signaling in the heart is inhibited by GCA.

Many studies have demonstrated a functional link between Ang II and TGF-β1 in the heart, and both are potent inducers of cardiac hypertrophy. Ang II has been shown to induce the expression of TGF-β1 in cardiac myocytes and fibroblasts (26). The absence of the TGF-β1 gene prevented the development of cardiac hypertrophy in response to subpressor doses of Ang II (27). We have demonstrated previously that genetic or pharmacological blockade of AT1 suppressed cardiac TGF-β1 overexpression and attenuated cardiac hypertrophy in GCA-deficient mice (6, 7). It has also been demonstrated that pharmacological blockade of AT2 is able to attenuate Ang II-stimulated TGF-β1 secretion in valvular interstitial cells (28). In the present study, overexpression of TGF-β1 in GCA deficiency was modulated by deletion of AT2, which also diminished the extent of cardiac hypertrophy. Thus, the present findings suggest that cardiac TGF-β1 participates in GCA-elicited inhibition of AT2-mediated pro-hypertrophic signaling in the heart.

Genetic deletion and pharmacological blockade of AT1 both reversed cardiac hypertrophy in GCA KO mice, thus implicating AT1 in growth promotion (6). Ablation of AT2 in the present study also partially attenuated cardiac hypertrophy in GCA KO mice, but somewhat surprisingly, the AT1 antagonist olmesartan did not produce further decreases in the HW/BW or LVW/BW ratios despite exerting beneficial effects on SBP. Importantly, however, it has been reported that blockade of AT2 abolished the anti-hypertrophic effect of AT1 antagonists in hearts of aged rats (29) and that combined AT1/AT2 blockade did not influence Ang II infusion-dependent cardiac hypertrophy in Sprague Dawley rats (30). The implication of these studies in intact animals, that AT2 is essential for the anti-hypertrophic effects of AT1 antagonists, is supported by the present findings in gene-targeted animals.

The present study further distinguishes the impact of pharmacological AT1 antagonism on SBP from effects on cardiac remodeling. Thus, olmesartan decreased SBP in intact, GCA-null, AT2-null, and GCA/AT2-double null mice, whereas cardiac hypertrophy was reversed by olmesartan only in GCA KO mice. Ang II signaling leading to altered gene transcriptional activation and function may involve multiple intracellular pathways. The AT1 is coupled to heterotrimeric G proteins and may activate phospholipases to increase calmodulin kinase activity and calcium release, which effects vasoconstriction (31). Balanced against this is the activation of ANP and BNP transcription and cross talk with the AT2, which modulate hypertensive actions (31). On the other hand, cardiomyocyte proliferation and hypertrophy are also stimulated by Ang II acting via AT1 signaling through the epidermal growth factor receptor coupled to MAPKs (32, 33). Thus, the present observations that cardiac hypertrophy in GCA deficiency is independent of blood pressure reg-

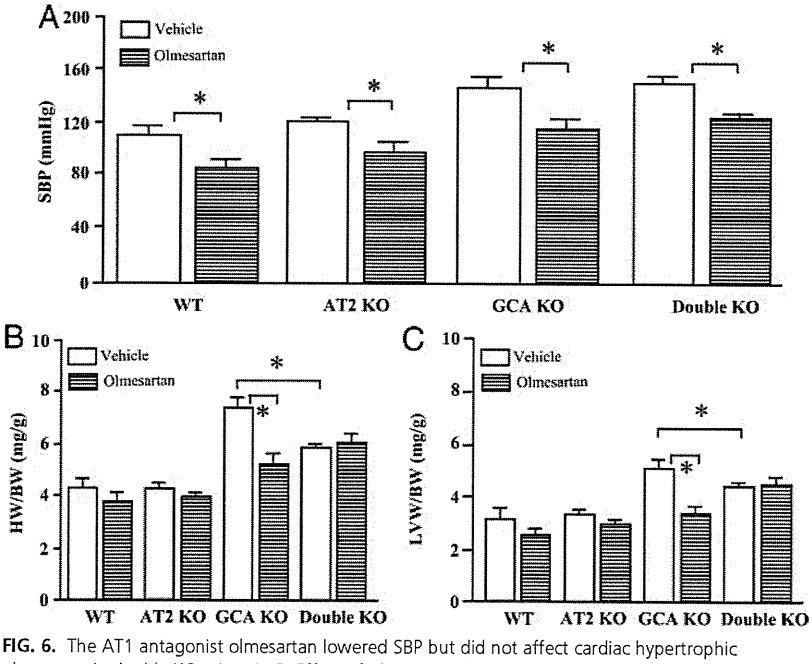

FIG. 6. The AT1 antagonist olmesartan lowered SBP but did not affect cardiac hypertrophic phenotype in double KO mice. A–C, Effect of olmesartan (10 mg/kg orally for 4 wk) on SBP (A), HW/BW (B), and LVW/BW (C) in hearts of mice carrying each of the genotypes under investigation. Values are means ± SEM (n = 7–9). *, $P < 0.05$.

ulation is consistent with the differential activation of alternate signaling cascades by AT1 and AT2.

Recently, several lines of evidence have suggested that GCA activity is relatively decreased in certain populations of patients with cardiovascular diseases. A functional polymorphism in the 5′-flanking region of the human GCA gene that is associated with essential hypertension and cardiac hypertrophy has been described (34). This variant most likely diminishes GCA gene expression in these patients, predisposing them to hypertension and cardiac hypertrophy such as that observed in GCA-deficient mice. Another polymorphism in the human GCA gene 5′-flank modulates left ventricular mass in essential hypertension (35). We also reported that a further polymorphism in the GCA 5′-flanking region, which decreases the transactivation of the GCA promoter in vascular smooth muscle cells, is associated with essential hypertension (36). Furthermore, it is emerging that desensitization of GCA signaling occurs in patients with severe heart failure (37, 38). These lines of evidence suggest that functional deterioration of GCA signaling may contribute to the progression of certain cardiovascular diseases. At this time, it is unclear whether an AT2-dependent mechanism could be operative in these patients. The present findings that cardiac hypertrophy in GCA-null mice is attenuated by blocking AT2 may provide important information for further detailed mechanistic research and eventual application of AT2 antagonists in patients with hypertension and cardiac hypertrophy caused by decreased GCA activity.

Taken together, the present findings demonstrate that GCA inhibits AT2-mediated cardiac growth-promoting signaling pathways and provides new insights into endogenous protective mechanisms against cardiac remodeling.

Acknowledgments

We thank Dr. Akiyoshi Fukamizu (University of Tsukuba, Tsukuba, Ibaraki, Japan) for the AT1a-deficient mice and Dr. David L. Garbers (Howard Hughes Medical Institute and Department of Pharmacology, University of Texas, Southwestern Medical Center at Dallas, Dallas, TX) for GCA-deficient mice.

Address all correspondence and requests for reprints to: Yuhao Li, 54 Kawahara-cho, Shogoin, Sakyo-ku, Kyoto 606-8507, Japan. E-mail: yuhao@kuhp.kyoto-u.ac.jp.

This work was supported in part by research grants from Japanese Ministry of Education, Science and Culture, the Japanese Ministry of Health and Welfare and the Japanese Society for the Promotion of Science.

Disclosure Summary: The authors have nothing to declare.

References

1. Gosse P 2005 Left ventricular hypertrophy as a predictor of cardiovascular risk. J Hypertens Suppl 23:S27–S33
2. Nakao K, Itoh H, Saito Y, Mukoyama M, Ogawa Y 1996 The natriuretic peptide family. Curr Opin Nephrol Hypertens 5:4–11
3. Horio T, Nishikimi T, Yoshihara F, Matsuo H, Takishita S, Kangawa K 2000 Inhibitory regulation of hypertrophy by endogenous atrial natriuretic peptide in cultured cardiac myocytes. Hypertension 35:19–24
4. Ogawa Y, Tamura N, Chusho H, Nakao K 2001 Brain natriuretic peptide appears to act locally as an antifibrotic factor in the heart. Can J Physiol Pharmacol 79:723–729
5. Lopez MJ, Wong SK, Kishimoto I, Dubois S, Mach V, Friesen J, Garbers DL, Beuve A 1995 Salt-resistant hypertension in mice lacking the guanylyl cyclase-A receptor for atrial natriuretic peptide. Nature 378:65–68
6. Li Y, Kishimoto I, Saito Y, Harada M, Kuwahara K, Izumi T, Takahashi N, Kawakami R, Tanimoto K, Nakagawa Y, Nakanishi M, Adachi Y, Garbers DL, Fukamizu A, Nakao K 2002 Guanylyl cyclase A inhibits angiotensin II type 1a receptor-mediated cardiac remodeling, an endogenous protective mechanism in the heart. Circulation 106:1722–1728
7. Li Y, Kishimoto I, Saito Y, Harada M, Kuwahara K, Izumi T, Hamanaka I, Takahashi N, Kawakami R, Tanimoto K, Nakagawa Y, Nakanishi M, Adachi Y, Garbers DL, Fukamizu A, Nakao K 2004 Androgen contributes to gender-related cardiac hypertrophy and fibrosis in mice lacking the gene encoding guanylyl cyclase-A. Endocrinology 145:951–958
8. Nakanishi M, Saito Y, Kishimoto I, Harada M, Kuwahara K, Takahashi N, Kawakami R, Nakagawa Y, Tanimoto K, Yasuno S, Usami S, Li Y, Adachi Y, Fukamizu A, Garbers DL, Nakao K 2005 Role of natriuretic peptide receptor GC-A in myocardial infarction evaluated using genetically engineered mice. Hypertension 46:441–447
9. Hunyady L, Turu G 2004 The role of the AT1 angiotensin receptor in cardiac hypertrophy: angiotensin II receptor or stretch sensor? Trends Endocrinol Metab 15:405–408
10. Berry C, Touyz R, Dominiczak AF, Webb RC, Johns DG 2001 Angiotensin receptors: signaling, vascular pathophysiology, and interactions with ceramide. Am J Physiol Heart Circ Physiol 281:H2337–H2365
11. Lopez JJ, Lorell BH, Ingelfinger JR, Weinberg EO, Schunkert H, Diamant D, Tang SS 1994 Distribution and function of cardiac angiotensin AT1- and AT2-receptor subtypes in hypertrophied rat hearts. Am J Physiol 267:H844–H852
12. Suzuki J, Matsubara H, Urakami M, Inada M 1993 Rat angiotensin II (type 1A) receptor mRNA regulation and subtype expression in myocardial growth and hypertrophy. Circ Res 73:439–447
13. Tsutsumi Y, Matsubara H, Ohkubo N, Mori Y, Nozawa Y, Murasawa S, Kijima K, Maruyama K, Masaki H, Moriguchi Y, Shibasaki Y, Kamihata H, Inada M, Iwasaka T 1998 Angiotensin II type 2 receptor is upregulated in human heart with interstitial fibrosis, and cardiac fibroblasts are the major cell type for its expression. Circ Res 83:1035–1046
14. Mifune M, Sasamura H, Shimizu-Hirota R, Miyazaki H, Saruta T 2000 Angiotensin II type 2 receptors stimulate collagen synthesis in cultured vascular smooth muscle cells. Hypertension 36:845–850
15. Senbonmatsu T, Ichihara S Price Jr E, Gaffney FA, Inagami T 2000 Evidence for angiotensin II type 2 receptor-mediated cardiac myocyte enlargement during *in vivo* pressure overload. J Clin Invest 106:R25–R29
16. Ichihara S, Senbonmatsu T, Price Jr E, Ichiki T, Gaffney FA, Inagami T 2001 Angiotensin type 2 receptor is essential for ventricular hypertrophy and cardiac fibrosis in chronic angiotensin II-induced hypertension. Circulation 104:346–351
17. Yan X, Price RL, Nakayama M, Ito K, Schuldt AJ, Manning WJ, Sanbe A, Borg TK, Robbins J, Lorell BH 2003 Ventricular-specific expression of angiotensin II type 2 receptors causes dilated cardiomyopathy and heart failure in transgenic mice. Am J Physiol Heart Circ Physiol 285:H2179–H2187
18. D'Amore A, Black MJ, Thomas WG 2005 The angiotensin II type 2 receptor causes constitutive growth of cardiomyocytes and does not antagonize angiotensin II type 1 receptor-mediated hypertrophy. Hypertension 46:1347–1354
19. Sanada S, Node K, Minamino T, Takashima S, Ogai A, Asanuma H, Ogita H, Liao Y, Asakura M, Kim J, Hori M, Kitakaze M 2003 Long-acting Ca^{2+} blockers prevent myocardial remodeling induced by chronic NO inhibition in rats. Hypertension 41:963–967
20. Lorenzo O, Ruiz-Ortega M, Suzuki Y, Rupérez M, Esteban V, Sugaya T, Egido J 2002 Angiotensin III activates nuclear transcription factor-κB in cultured mesangial cells mainly via AT_2 receptors: studies with AT_1 receptor-knockout mice. J Am Soc Nephrol 13:1162–1171
21. Akishita M, Iwai M, Wu L, Zhang L, Ouchi Y, Dzau VJ, Horiuchi M 2000 Inhibitory effect of angiotensin II type 2 receptor on coronary arterial remodeling after aortic banding in mice. Circulation 102:1684–1689
22. de Bold AJ, Bruneau BG, Kuroski de Bold ML 1996 Mechanical and neuroendocrine regulation of the endocrine heart. Cardiovasc Res 31:7–18
23. Masaki H, Kurihara T, Yamaki A, Inomata N, Nozawa Y, Mori Y, Murasawa S, Kizima K, Maruyama K, Horiuchi M, Dzau VJ, Takahashi H, Iwasaka T, Inada M, Matsubara H 1998 Cardiac-specific overexpression of angiotensin II AT2 receptor causes attenuated response to AT1 receptor-mediated pressor and chronotropic effects. J Clin Invest 101:527–535

24. Inagami T, Senbonmatsu T 2001 Dual effects of angiotensin II type 2 receptor on cardiovascular hypertrophy. Trends Cardiovasc Med 11:324–328
25. Oliviéro P, Chassagne C, Kolar F, Adamy C, Marotte F, Samuel JL, Rappaport L, Ostadal B 2000 Effect of pressure overload on angiotensin receptor expression in the rat heart during early postnatal life. J Mol Cell Cardiol 32:1631–1645
26. Rosenkranz S 2004 TGF-β1 and angiotensin networking in cardiac remodeling. Cardiovasc Res 63:423–432
27. Schultz Jel J, Witt SA, Glascock BJ, Nieman ML, Reiser PJ, Nix SL, Kimball TR, Doetschman T 2002 TGF-β1 mediates the hypertrophic cardiomyocyte growth induced by angiotensin II. J Clin Invest 109:787–796
28. Scott L, Kerr A, Haydock D, Merrilees M 1997 Subendothelial proteoglycan synthesis and transforming growth factor β distribution correlate with susceptibility to atherosclerosis. J Vasc Res 34:365–377
29. Jones ES, Black MJ, Widdop RE 2004 Angiotensin AT2 receptor contributes to cardiovascular remodelling of aged rats during chronic AT1 receptor blockade. J Mol Cell Cardiol 37:1023–1030
30. Brassard P, Amiri F, Schiffrin EL 2005 Combined angiotensin II type 1 and type 2 receptor blockade on vascular remodeling and matrix metalloproteinases in resistance arteries. Hypertension 46:598–606
31. Berry C, Touyz R, Dominiczak AF, Webb RC, Johns DG 2001 Angiotensin receptors: signaling, vascular pathophysiology, and interactions with ceramide. Am J Physiol Heart Circ Physiol 281:H2337–H2365
32. Kim S, Iwao H 2000 Molecular and cellular mechanisms of angiotensin II-mediated cardiovascular and renal diseases. Pharmacol Rev 52:11–34
33. Thomas WG, Brandenburger Y, Autelitano DJ, Pham T, Qian H, Hannan RD 2002 Adenoviral-directed expression of the type 1A angiotensin receptor promotes cardiomyocyte hypertrophy via transactivation of the epidermal growth factor receptor. Circ Res 90:135–142
34. Nakayama T, Soma M, Takahashi Y, Rehemudula D, Kanmatsuse K, Furuya K 2000 Functional deletion mutation of the 5′-flanking region of type A human natriuretic peptide receptor gene and its association with essential hypertension and left ventricular hypertrophy in the Japanese. Circ Res 86:841–845
35. Rubattu S, Bigatti G, Evangelista A, Lanzani C, Stanzione R, Zagato L, Manunta P, Marchitti S, Venturelli V, Bianchi G, Volpe M, Stella P 2006 Association of atrial natriuretic peptide and type A natriuretic peptide receptor gene polymorphisms with left ventricular mass in human essential hypertension. J Am Coll Cardiol 48:499–505
36. Usami S, Kishimoto I, Saito Y, Harada M, Kuwahara K, Nakagawa Y, Nakanishi M, Yasuno S, Kangawa K, Nakao K 2008 Association of CT dinucleotide repeat polymorphism in the 5′-flanking region of the guanylyl cyclase (GC)-A gene with essential hypertension in the Japanese. Hypertens Res 31:89–96
37. Tsutamoto T, Kanamori T, Wada A, Kinoshita M 1992 Uncoupling of atrial natriuretic peptide extraction and cyclic guanosine monophosphate production in the pulmonary circulation in patients with severe heart failure. J Am Coll Cardiol 20:541–546
38. Tsutamoto T, Kanamori T, Morigami N, Sugimoto Y, Yamaoka O, Kinoshita M 1993 Possibility of down-regulation of atrial natriuretic peptide receptor coupled to guanylate cyclase in peripheral vascular beds of patients with chronic severe heart failure. Circulation 87:70–75